International Journal of Earth Sciences (2022) 111:2633–2656
https://doi.org/10.1007/s00531-021-02148-z

ORIGINAL PAPER

Field geology and provenance analyses of the Ganqimaodu accretionary complex (Inner Mongolia, China): implications for early Paleozoic tectonic evolution of the southern Central Asian Orogenic Belt

Hao Zeng[1,2,3] · Dongfang Song[1,2,3] · Wenjiao Xiao[4,3] · Puqing Li[1,2,3]

Received: 24 August 2021 / Accepted: 1 December 2021 / Published online: 22 January 2022

Abstract
The early Paleozoic accretionary architecture of the Alxa and Bainaimiao regions in southern Central Asian Orogenic Belt (CAOB) is still ambiguous. In particular, the subduction polarity and tectonic origin of the Bainaimiao Arc are intensely controversial. The Ganqimaodu area in Inner Mongolia provides an excellent window to address this issue. This study presents field and detrital zircon U–Pb–Hf isotopic data of Paleozoic (meta)sedimentary rocks from Ganqimaodu to investigate their provenance and tectonic settings. New field observations show that both the Ondor sum and Hadahushu groups are composed of slightly metamorphosed flysch deposits with pervasive occurrence of "block-in-matrix" structure and isoclinal folds. Two chlorite–quartz schists from the Ondor sum Group yield age peaks at ~ 425, ~ 966, ~ 1590, ~ 1930 and ~ 2564 Ma, and three sandstones from the Hadahushu Group display similar age spectrums with peaks at ~ 443, ~ 586, ~ 960, ~ 1473, ~ 1765 and ~ 2480 Ma. New detrital zircon ages constrain the maximum depositional ages of the Ondor sum and Hadahushu groups to Early Devonian. The Ondor sum and Hadahushu groups are here interpreted as an accretionary complex due to northward subduction of the South Bainaimiao Ocean based on field data and provenance analyses. Our new results combined with previous data suggest bidirectional subduction for the western segment of the South Bainaimiao Ocean during Late Cambrian to Early Devonian. We advocate an archipelago with accretionary complexes, continental fragments, and magmatic arcs for the architecture of the southern CAOB during early Paleozoic, an analogous to modern southwest Pacific accretionary system.

Keywords Accretionary complex · Detrital zircon U–Pb · Provenance · Alxa · Central Asian Orogenic Belt

Introduction

Accretionary orogens are formed through continuous oceanic lithosphere subduction at the convergent plate margins, which have played an irreplaceable role in continental growth throughout Earth's history (Cawood et al. 2009; Condie 2007). The Central Asian Orogenic Belt (CAOB, or Altaids), surrounded by the Baltica Craton to the northwest, the Siberian Craton to the north, and the Karakum, Tarim, and North China cratons to the south, is considered as one of the largest Phanerozoic accretionary orogens in the world (Fig. 1; Jahn et al. 2000; Şengör and Natal'in 1996; Şengör et al. 1993; Windley et al. 2007; Xiao et al. 2015a). The CAOB has undergone ~ 800 Ma tectonic evolution from Neoproterozoic to Early Mesozoic (Khain et al. 2002; Kröner et al. 2007; Xiao et al. 2009), and was built

✉ Dongfang Song
dfsong@mail.iggcas.ac.cn

1 State Key Laboratory of Lithospheric Evolution, Institute of Geology and Geophysics, Chinese Academy of Sciences, Beijing 100029, China

2 Innovation Academy for Earth Science, Chinese Academy of Sciences, Beijing 100029, China

3 College of Earth and Planetary Sciences, University of Chinese Academy of Sciences, Beijing 100049, China

4 Xinjiang Research Centre for Mineral Resources, Xinjiang Institute of Ecology and Geography, Chinese Academy of Sciences, Urumqi 830011, China

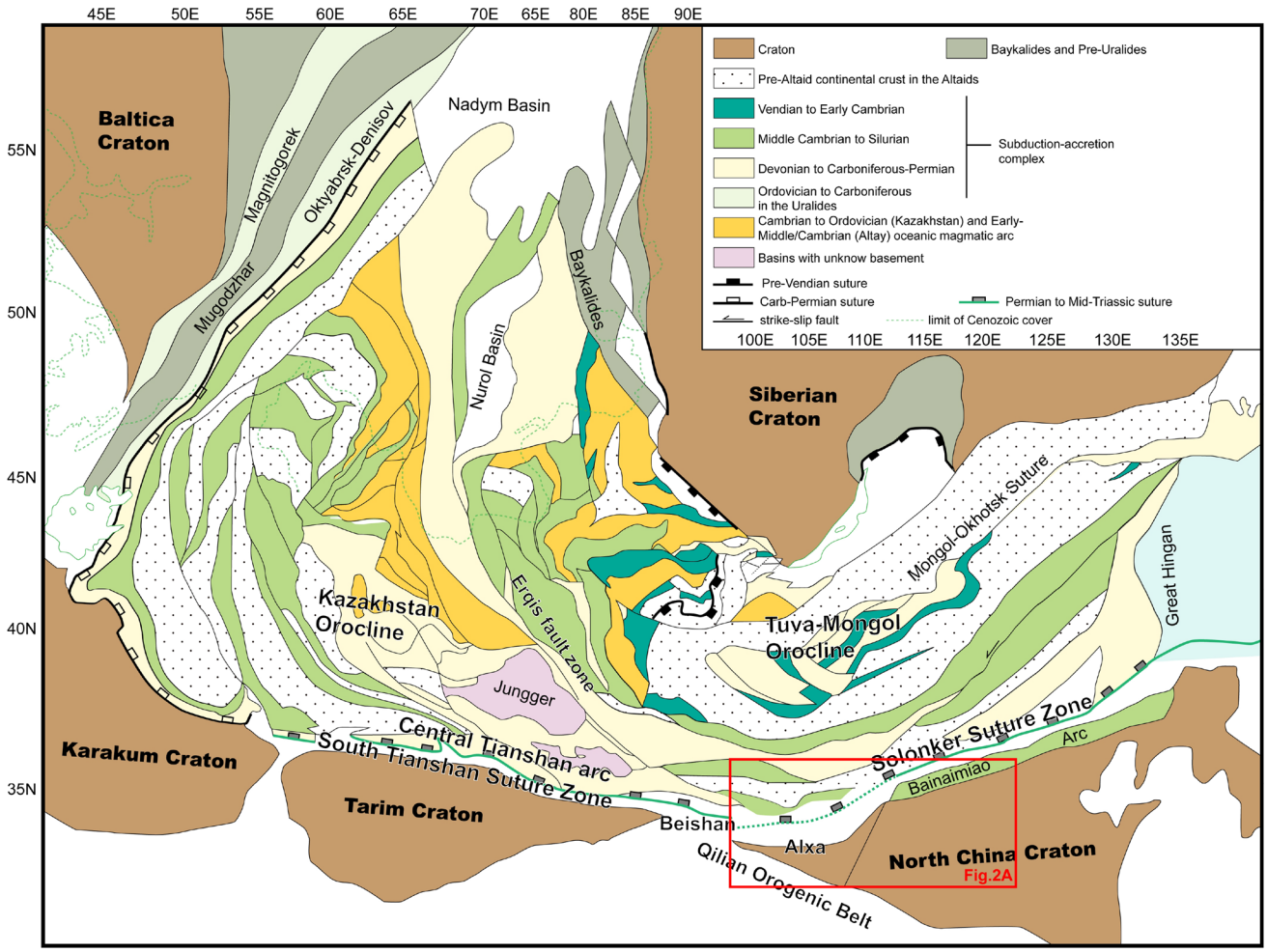

Fig. 1 Tectonic map of Central Asian Orogenic Belt and its surrounding cratons (modified after Şengör and Natal'in 1996, Xiao et al. 2015a, Song et al. 2018 and Zhang et al. 2014), showing the spatial–temporal distribution characteristics of the main tectonic units in the Central Asian Orogenic Belt. Along the southernmost Central Asian Orogenic Belt, the major tectonic zones include Central Tianshan Arc, South Tianshan Suture Zone, Beishan, Alxa, Solonker Suture Zone and Bainaimiao Arc from west to east

by sustaining accretion of subduction–accretion complexes, magmatic arcs, arc-related basins, ophiolites, seamounts, and continental fragments during the subduction and final closure of the Paleo-Asian Ocean (PAO) (Kröner et al. 2007; Safonova et al. 2017; Windley et al. 2007; Xiao et al. 2015a; Zhou et al. 2018c). The South Tianshan, Beishan, Alxa, and Solonker sutures along the southernmost CAOB have been considered as the position for the final closure of the PAO, and a large number of studies have focused on the Late Paleozoic–Early Mesozoic tectonic evolution of these regions to constrain the terminal amalgamation of the CAOB (Liu et al. 2017b; Xiao et al. 2003, 2009, 2013; Zhang et al. 2013c).

The Alxa Tectonic Belt, situated between the Beishan orogen in the west and the Solonker suture zone in the east (Fig. 1), contains abundant Late Paleozoic magmatic–sedimentary records and ophiolitic mélanges related to amalgamation of the southern CAOB (Feng et al. 2013; Song et al. 2019, 2018; Zheng et al. 2014). However, the Early Paleozoic tectonic evolutionary history of the Alxa Tectonic Belt is largely unknown. Early Paleozoic strata in the Zhusileng and Hangwula areas in the northern Alxa were considered as passive continental margin deposits (Wu and He 1993). Zheng et al. (2016) reported Silurian intrusions from the Engger Us area, and interpreted them as arc magmatism. Ordovician to Early Devonian arc-related plutons in the southwestern Alxa were considered to be related to southward subduction of the PAO (Liu et al. 2016b). The Early Paleozoic tectonic history of the Alxa Tectonic Belt needs further constraints by comparing with adjacent regions. To the east of the Alxa Tectonic Belt, an Early Paleozoic magmatic arc belt, the Bainaimiao Arc, developed between the Solonker suture zone to the north and the North China Craton to the south (Xiao et al. 2003; Fig. 2). However, intense controversies remain on the subduction polarity and

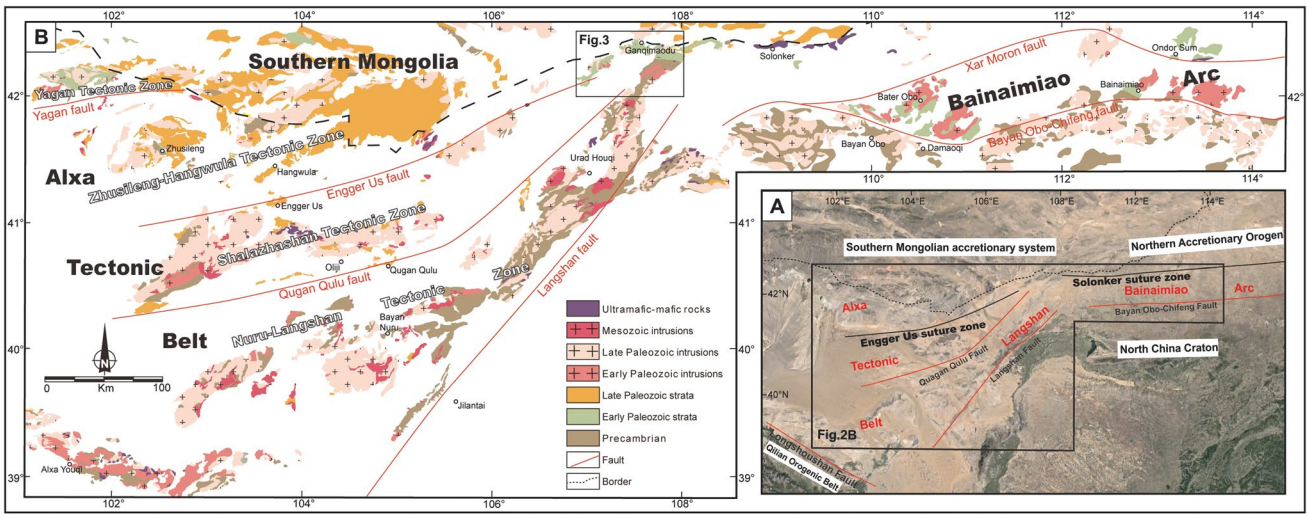

Fig. 2 **A** Tectonic map of southeastern part of Central Asian Orogenic Belt and adjacent regions showing situations of the major tectonic units including the Southern Mongolian Collage System, the Northern Accretionary Orogen, the Engger Us Suture Zone, the Solonker Suture Zone, the Alxa Tectonic Belt, the Bainaimiao Arc, the Qilian Orogenic Belt and the North China Craton. **B** Simplified geological map of Alxa-northern margin of the North China Craton showing major lithostratigraphic composition. The location of the study area of Fig. 3 is indicated. Modified from Liu et al. (2016b), Liu et al. (2020), Guy et al. (2014) and Taylor et al. (2013)

tectonic origin of the Bainaimiao Arc, including the southward subduction of the Paleo-Asian Ocean evidenced by Ondor sum subduction–accretion complexes to the north of the Bainaimiao Arc (Xiao et al. 2003), or the northward subduction of the South Bainaimiao Ocean supported by the Wude–Chegandalai ophiolitic mélanges to the south of it (Zhang et al. 2014). The along-strike tectonic correlation between the Alxa Tectonic Belt and the Bainaimiao Arc is important for a better understanding of the Early Paleozoic tectonic evolution of the eastern segment of the southern CAOB.

The Ganqimaodu area connects the Alxa Tectonic Belt with the Bainaimiao Arc along the southern CAOB (Fig. 2B). It consists mainly of early Paleozoic igneous rocks, (meta)sedimentary rocks and ophiolitic mélanges (Anonymous 1980a, b; Xu et al. 2013; Fig. 3). The tectonic setting of early Paleozoic strata in the Ganqimaodu area is still unclear and is intensely debated. Xu et al. (2013) suggested that the Ordovician–Silurian Ondor sum Group represents the passive margin deposition of the Hunshandake Block and the early–middle Silurian Hadahushu Group deposited in a collision-related foreland basin. However, Xiao et al. (2003) interpreted the Ondor sum Group as subduction–accretion complexes by southward subduction of the PAO. The Hadahushu Group was also suggested as back-arc basin deposition above the south-dipping subduction zone beneath the North China Craton (Tian et al. 2019e). In this study, we integrate field geology with zircon U–Pb–Hf isotopic analyses for (meta)sedimentary rocks from the Ganqimaodu area to determine their provenance and tectonic setting. Our new data combined with previous studies provide invaluable information for the early Paleozoic tectonic framework and accretionary process of the southern CAOB.

Geologic background

The Ganqimaodu area

The Ganqimaodu area is located in a key position in the southern CAOB connecting the Southern Mongolian accretionary system to the north, the Alxa Tectonic Belt to the southwest, and the Bainaimiao Arc to the east (Figs. 2B; 3). According to Anonymous (1980a, b), strata in the Ganqimaodu area mainly include: Mesoproterozoic quartzite, marble and garnet schist, Early–Middle Paleozoic Ondor sum Group greenschist-facies clastic rocks, Early–Middle Silurian slightly metamorphic sedimentary rocks (the Hadahushu Group), and a small amount of Carboniferous–Permian strata. Recent detrital zircon U–Pb dating indicate that the Ondor sum Group was deposited in the early Paleozoic, with the lower part at 470–455 Ma and the upper part at 455–415 Ma (Xu et al. 2016). The Silurian Hadahushu Group was suggested to be deposited after early Silurian (~438 Ma) (Tian et al. 2019e). Numerous Mesoproterozoic to Late Paleozoic plutons intruded into these strata (Anonymous 1980a; Sun et al. 2013, 2018). Early Paleozoic intrusions in the Ganqimaodu area were considered as products of the southward subduction of the PAO beneath the North China Craton (Xu et al. 2013; Zhang et al. 2019b).

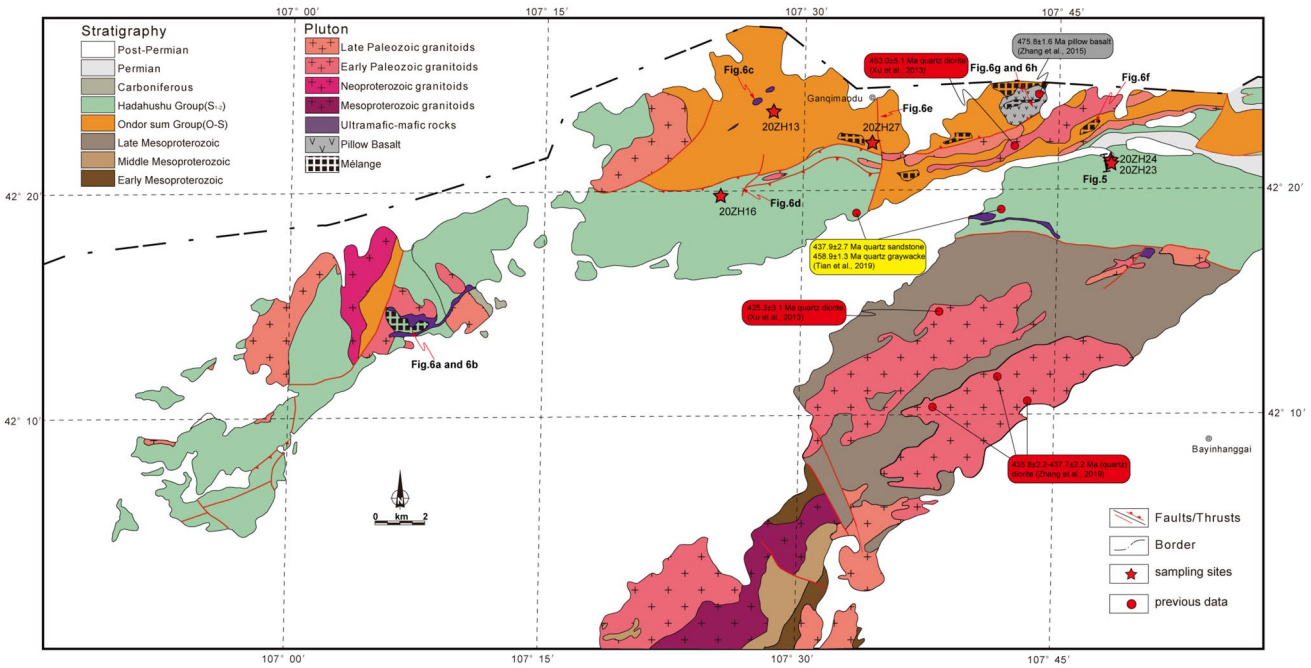

Fig. 3 Detailed geological map of the Ganqimaodu area (modified from Anonymous 1980a, b Xu et al. 2013 and personal field observation). Previous data are from Tian et al. (2019e), Xu et al. (2013), Zhang et al. (2015) and Zhang et al. (2019b)

The Alxa Tectonic Belt

The Alxa Tectonic Belt (Fig. 2A, B) is a triangle-shaped region separated from the North China Craton to the east by the Langshan fault and from the Qilian Orogenic Belt to the southwest by the Longshoushan thrust. To the north, the Alxa Tectonic Belt connects the Southern Mongolian accretionary system. Three main faults in the Alxa Tectonic Belt are: the Yagan fault, the Engger Us fault, and the Quagan Qulu fault (Wu and He 1993). These faults divide the Alxa Tectonic Belt into four tectonic zones: Yagan, Zhusileng–Hangwula, Shalazhashan, and Nuru–Langshan.

The Yagan Tectonic Zone lies to the north of the Yagan fault. Neoproterozoic strata consisting of marble and metasandstone in the northeast of Ejin Banner were intruded by a Neoproterozoic (~ 889 Ma) highly fractionated potassium-rich granite (Zhang et al. 2016b). The Middle Ordovician intermediate-basic to intermediate-acid volcanic rocks may represent an intra-oceanic arc (Wu and He 1993). There are also thick Late Paleozoic volcanic–sedimentary successions which were emplaced by numerous Carboniferous–Permian granitoids (Zhang et al. 2017b; Zheng et al. 2013).

Between the Yagan fault and Engger Us fault is the Zhusileng–Hangwula Tectonic Zone. This zone contains relatively complete strata from Neoproterozoic to Mesozoic with intense magmatism during the Late Paleozoic (Fei et al. 2019). A few Neoproterozoic granitoids have recently been reported (Wang et al. 2001; Zhou et al. 2013). Early Paleozoic strata composed of shallow-marine clastic rocks were previously considered as passive continental margin deposition, but recent detrital zircon studies suggested that the provenance of Ordovician to Devonian strata might be the northern microcontinents or arcs in the southern CAOB (Chen et al. 2019; Yin et al. 2015).

The Shalazhashan Tectonic Zone, located between the Engger Us fault to the north and the Quagan Qulu fault to the south, is mainly composed of Permian intrusions and Carboniferous–Permian volcanic and sedimentary rocks (Shi et al. 2014, 2018; Yin et al. 2016; Zhang et al. 2013c). A Mesoproterozoic (~ 1.4 Ga) orthogneiss has been reported in this tectonic zone (Shi et al. 2016).

The Nuru–Langshan Tectonic Zone contains numerous Precambrian rocks that comprise orthogneiss and paragneiss, indicating multi-phase magmatic–metamorphic events from Neoarchean to Neoproterozoic (Dan et al. 2012, 2014b; Gong et al. 2016; Shen et al. 2005; Song et al. 2017; Wu et al. 2014; Zhang et al. 2013a). A few metamorphic intrusions from the Langshan area have been reported, including 2.7–2.56 Ga granitic gneisses, 1.71–1.64 Ga metamorphic granites, and 914–908 Ma mafic intrusions (Bao et al. 2019; Liu 2012; Sun et al. 2018; Wang et al. 2016a). The Langshan Group consist of greenschist-facies metamorphosed clastic rocks, carbonate rocks, and interbedded volcanic rocks. Previous studies showed that the Langshan Group was deposited from ~ 1187 to 804 Ma (Hu et al. 2014; Liu et al. 2019a;

Tian et al. d). Ordovician–Silurian diorites and granitoid intrusions were interpreted as resulting from southward subduction of the PAO (Dan et al. 2016; Liu et al. 2016b; Teng et al. 2019; Tian et al. 2019a, 2019c; Wang et al. 2015b). A large number of plutons were emplaced in the Carboniferous–Permian, including gabbros, diorites, granodiorites, and granitoids (Dan et al. 2014a; Feng et al. 2013; Liu et al. 2016a, 2017b, 2019b; Song et al. 2019; Tian et al. 2019b; Wang et al. 2015b). Although early Paleozoic strata are lacking in this area, a few late Paleozoic volcanic–sedimentary rocks from the Beidashan area in the southwest of this zone may provide a key constraint for the final subduction processes of the PAO (Song et al. 2018).

Ophiolitic mélanges with block-in-matrix structure are distributed along both the Engger Us and Qugan Qulu faults. Based on geochronological and geochemical studies of exotic blocks within the ophiolitic mélanges, Zheng et al. (2014) suggested that the Engger Us ophiolite represents the Late Paleozoic main suture of the PAO, while Qugan Qulu ophiolite formed in a back-arc basin. The Yagan fault extends about 100 km from west to east in the Alxa region, but most of it is covered by Badain Jaran Deser (Wu and He 1993).

The Bainaimiao Arc

The Bainaimiao Arc (Fig. 2A, B) is situated on the northern margin of the North China Craton bounded by the E–W-trending Bayan Obo-Chifeng fault. The Bainaimiao Arc is dominated by early Paleozoic magmatic and sedimentary rocks with minor amounts of Precambrian rocks. Zircon Hf isotopic data (εHf(t) values vary from − 9.3 to 11.4; two-stage Hf model ages are mainly 0.7–1.29 Ga and 1.39–2.0 Ga) from these early Paleozoic magmatic rocks and Proterozoic detrital zircons (ca. 0.6–1.2 Ga and 1.3–2.0 Ga) from contemporaneous (meta)sedimentary rocks indicate that the Bainaimiao Arc was built on a Precambrian basement (Chen et al. 2020; Zhang et al. 2014; Zhou et al. 2018b, 2020). However, the tectonic affinity of the basement for the Bainiamiao Arc is still controversial. Most scholars considered that the Bainaimiao Arc is a continental arc on the North China Craton related to the southward subduction of the PAO (Xiao et al. 2003; Xu et al. 2013), while others proposed that the basement of the Bainaimiao Arc has an affinity to the Tarim Craton (Zhang et al. 2014; Zhou et al. 2020). The early Paleozoic plutons in the Bainaimiao Arc can be roughly divided into two types based on their petrography and isotopic compositions: intrusions older than ~ 450 Ma are intermediate-basic with positive εHf(t) values, and those younger than ~ 450 Ma are intermediate-acidic with both positive and negative εHf(t) values (Liu et al. 2020). Early Paleozoic volcanic rocks include basalt, andesite, dacite, and tuff, which have been dated at ~ 518–404 Ma (Liu et al. 2003, 2013; Ma et al. 2019; Qian et al. 2017; Zhang et al. 2013b, 2014, 2017a, 2019a; Zhou et al. 2020). The εHf(t) values of these magmatic rocks generally decreased with decreasing age until ~ 415 Ma (Chen et al. 2020). Early Paleozoic strata are composed of Ordovician to Silurian metasedimentary rocks collectively termed the Baoerhantu Group and Bainaimiao Group (Zhang et al. 2014). The early Silurian Xuniwusu Formation represents a set of flysch deposition consisting of clastic rocks with carbonate and tuff interlayers (Zhang et al. 2017a). The latest Silurian–early Devonian Xibiehe Formation was considered as molasse deposition unconformably on the early Paleozoic ophiolitic mélanges, arc-related plutons, and sedimentary rocks of the Bainaimiao Arc (Wang et al. 2020; Zhang et al. 2010).

The Southern Mongolian accretionary system

The Southern Mongolian accretionary system here refers to the domain that lies to the south of the Main Mongolian Lineament (Fig. 2A). It is divisible into four zones from north to south: the Lake zone, the Gobi-Altai zone, the Trans-Altai zone, and the South Gobi zone. The Lake zone is mainly composed of Precambrian basement with Early Cambrian ophiolitic mélanges and eclogites and Cambrian-Ordovician arc-related magmatic rocks (Lehmann et al. 2010). The Gobi-Altai zone has a Cambrian crystalline basement unconformably overlain by a thick Early–Middle Ordovician sedimentary–volcanic sequence, followed by a Silurian–Devonian passive margin deposition which was intruded by Devonian–Permian Japan-type magmatic arc (Badarch et al. 2002; Lehmann et al. 2010). The Trans-Altai zone, separated from the Gobi-Altai zone by the Trans-Altai fault to the north and bounded by the Gobi-Tianshan fault to the south, largely consists of dismembered ophiolitic mélange containing serpentinized peridotite, gabbro and pillow basalt, overlain by Late Silurian–Early Devonian radiolarian cherts, andesitic and basaltic volcanic rocks and Middle Devonian to Carboniferous volcanic–sedimentary rocks (Badarch et al. 2002; Guy et al. 2014). The South Gobi zone occupies the southernmost part of Mongolia, separated from the Trans-Gobi zone by the Gobi-Tianshan fault. Badarch et al. (2002) classified this zone as a cratonal terrane with a Precambrian basement. Now it is considered as the South Mongolian Microcontinent evidenced by some Neoproterozoic granitoids or granitic gneisses (Wang et al. 2001; Yarmolyuk et al. 2005; Zhang et al. 2016b). Ordovician to Silurian siliceous clastic rocks, Early Devonian to Carboniferous volcanic and sedimentary rocks deposited extensively above the basement (Lehmann et al. 2010). However, Taylor et al. (2013) found that all so-called Precambrian metamorphic rocks formed from Carboniferous to Triassic based on zircon U–Pb dating, and argued that the Southern Mongolia is a Paleozoic arc rather than a microcontinent.

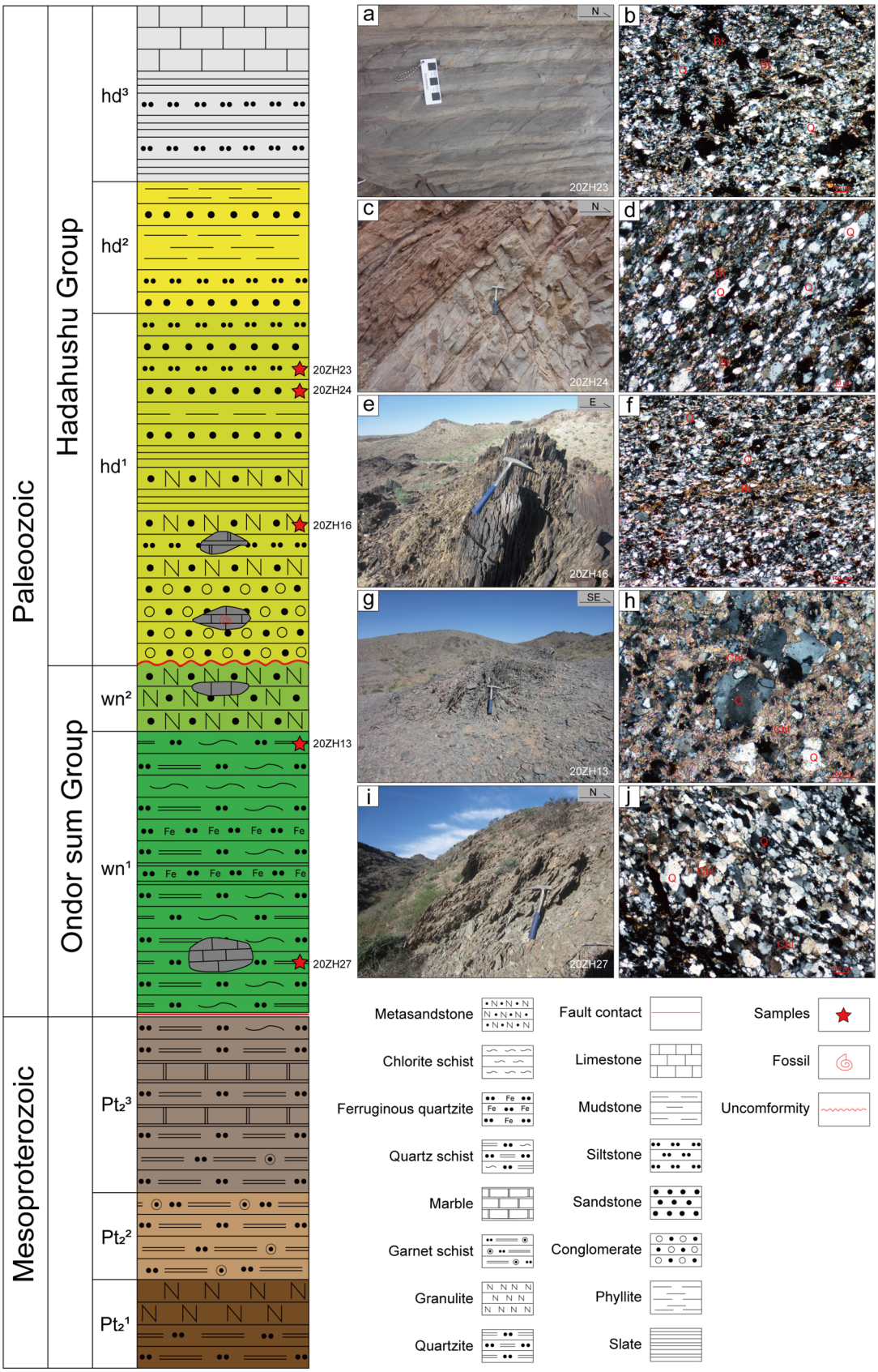
Paleoozoic
Mesoproterozoic
Hadahushu Group
Ondor sum Group
hd³
hd²
hd¹
wn²
wn¹
Pt₂³
Pt₂²
Pt₂¹
20ZH23
20ZH24
20ZH16
20ZH13
20ZH27
a
b
c
d
e
f
g
h
i
j
Metasandstone
Chlorite schist
Ferruginous quartzite
Quartz schist
Marble
Garnet schist
Granulite
Quartzite
Fault contact
Limestone
Mudstone
Siltstone
Sandstone
Conglomerate
Phyllite
Slate
Samples
Fossil
Uncomformity

◂**Fig. 4** Stratigraphic column of the Early Paleozoic strata in the Ganqimaodu area (modified from Anonymous (1980a,, b), Tian et al. (2019e) and our own observation). Field and microscopic photographs of these sedimentary rocks in the study area are shown: (**a**, **b**) sample 20ZH23, quartz sandstone; (**c**, **d**) sample 20ZH24, quartz sandstone; (**e**, **f**) sample 20ZH16, metamorphosed quartz sandstone; (**g**, **h**) sample 20ZH13, chlorite–quartz schist; (**i**, **j**) sample 20ZH27, chlorite–quartz schist. All microscopic photos are under cross-polarized light. *Q*, quartz; *Bt*, biotite; *Chl*, chlorite

Field geology, sampling and petrology

To investigate the early Paleozoic accretionary history of the southern CAOB, a systematic study including field geology and zircon U–Pb–Hf isotopic analyses were carried out for the early Paleozoic rocks in the Ganqimaodu region. The locations for sampling are indicated in Figs. 3 and 4.

The Hadahushu Group, unconformably overlying the Ondor sum Group (Xu et al. 2013), can be divided into three parts based on lithologic assemblages (Anonymous 1980a; b; Fig. 4): a lower part of conglomerate, slate, thin-bedded sandstone and siltstone, and limestone lenticles along with coral fossils; a middle part of interbedded sandstone and phyllite; an upper part of slate, limestone and siltstone. Ophiolitic mélanges are found within the lower part of the Hadahushu Group where limestone and basic volcanic rock blocks were wrapped in the (meta)sedimentary rocks (Fig. 6a, b, d). A ~ 180 m long measured section (Fig. 5) of the Hadahushu Group comprises interbedded sandstone, siltstone and mudstone. Three samples were collected from the lower part of the Silurian Hadahushu Group. Samples 20ZH23 (Fig. 4a, b) and 20ZH24 (Fig. 4c. d) are quartz sandstones from the cross section described above (Fig. 5). These sandstones mainly consist of quartz and biotite. Sample 20ZH16 (Fig. 4e, f) is a metamorphosed quartz sandstone and mainly composed of fine-grain quartz and biotite with NW dipping foliation.

According to Anonymous (1980a, b), the Ondor sum Group in the Ganqimaodu area are characterized by greenschist intercalated with quartzite and basic volcanic rock, and are divisible into the lower and upper parts with slightly lithologic variations (Fig. 4). The lower part primarily consists of chlorite–quartz schist, sericite–quartz schist and quartzite, and the upper part comprises metasandstone with small limestone lens. Ophiolitic mélanges also exist widely in the lower part of the Ondor sum Group strata, which contain abundant blocks such as ultramafic rocks, basic volcanic rocks, limestones, pillow basalts, and siliceous rocks (Fig. 6c, f, g, h). In addition, the Ondor sum Group is deformed strongly with a foliation dipping NNW (Fig. 6e). Two chlorite–quartz schists (Sample 20ZH13, Fig. 4g, h; and 20ZH27, Fig. 4i, j) mainly consisting of fine-grained quartz and minor chlorite are taken from the lower part of Ondor sum Group.

Analytical methods

Zircon U–Pb dating

Zircon grains were separated by conventional magnetic and heavy liquid methods and hand-picked under a binocular microscope. Then these grains were randomly selected to mounted on adhesive tape, followed by enclosing in epoxy resin and polishing to about one third to one half of their thickness. To understand the origin and internal structure of these zircons and to select the most suitable target spots for U–Pb dating and Hf isotopic analyses, Cathodoluminescence (CL) imaging was operated with a scanning electron microscope at the Institute of Geology and Geophysics, Chinese Academy of Sciences (IGGCAS) in Beijing.

Zircon U–Pb dating was carried out at the IGGCAS using an Agilent 7500a Quadrupole-ICP-MS with a GeoLasHD 193 nm ArF excimer laser-ablation system. The diameter of laser ablation spot is 32 μm with the density of energy of 4.0 J/cm^2 at 71.8 mJ output of energy. Each spot analysis comprised 20 s of gas background followed by 50 s of sample ablation. Zircon 91,500 was used as external standard for age calculation, which measured twice every ten analyses. NIST SRM 610 and ARM were used as external standard for concentration calculation and another reference zircon SA01 was analyzed as an unknown to monitor the quality of age date. The more instrumental settings and detailed analytical procedures can be found in Wu et al. (2007) and Xie et al. (2008). Isotopic concentrations and ratios were calculated using the GLITTER program (Macquarie University). Common Pb was corrected according to the method proposed by Andersen (2002). The age calculations and plotting of Concordia diagrams were made using ISOPLOT 3.0 (Ludwig 2003), and DensityPlotter 7.2 was used to generate probability density and kernel distributions (Vermeesch 2012). In this study, $^{207}Pb/^{206}Pb$ ages are reported for zircons older than 1000 Ma, while $^{206}Pb/^{238}U$ ages are reported for zircons younger than 1000 Ma.

Zircon Lu–Hf isotopic analysis

Zircon in situ Hf isotope analysis was carried out using a Resolution SE 193 laser-ablation system attached to a Thermo Fisher Scientific Neptune Plus MC-ICP-MS at Beijing ZKKY Technology Co., Ltd. Instrumental conditions and data acquisition protocols were described by Hou et al. (2007). Lu–Hf isotopic compositions were analyzed for zircons near the same locations where U–Pb analyses were carried out. A beam diameter of 44 μm was

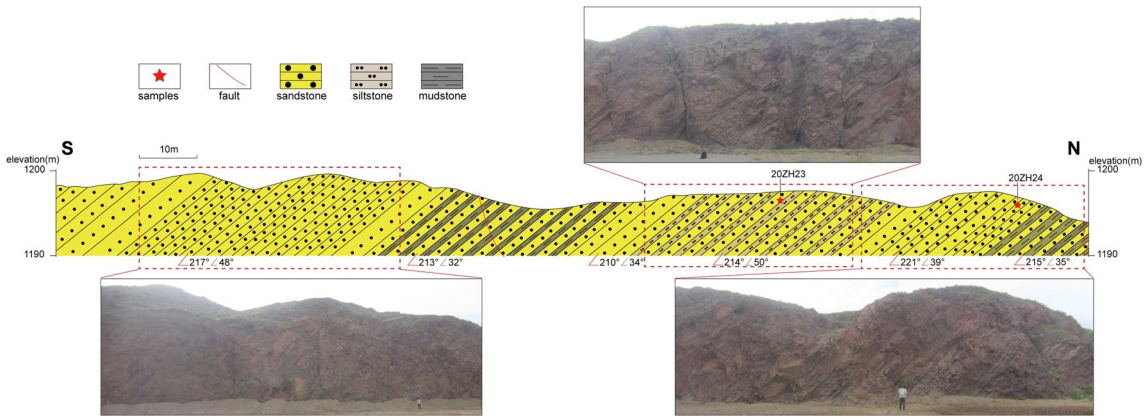

Fig. 5 Field features and sketch of stratum section of the Hadahushu Group flysch deposits. The location is indicated in Fig. 3

used for all the samples. The repetition rate was 10 Hz and the density of energy was 8 J/cm^2. As the carrier gas, Helium was used to transport the ablated material mixed with Argon from the laser-ablation cell to the MC-ICP-MS torch by a mixing chamber. Yb isotope ratios were normalized to $^{173}Yb/^{172}Yb = 1.35274$ and Hf isotope ratios were normalized to $^{179}Hf/^{177}Hf = 0.7325$ using an exponential law for instrumental mass bias correction (Wu et al. 2006). Due to the $^{176}Lu/^{177}Hf$ ratios in zircon is usually less than 0.002, the isobaric interference of ^{176}Hf isomers is mainly caused by ^{176}Yb, so the mean β_{Yb} value and the $^{176}Yb/^{172}Yb$ ratio of 0.5887 were applied for the Yb correction (Iizuka and Hirata 2005; Wu et al. 2006). Zircon international standard GJ-1 was used as the reference standard, with a weighted mean $^{176}Hf/^{177}Hf$ ratio of 0.282006 ± 21 (2σ, n = 16). The measured $^{176}Lu/^{177}Hf$ ratios and the ^{176}Lu decay constant of 1.867×10^{-11} yr^{-1} proposed by Söderlund et al. (2004) were used to calculate initial $^{176}Hf/^{177}Hf$ ratios. The present chondritic values of $^{176}Hf/^{177}Hf = 0.282772$ and $^{176}Lu/^{177}Hf = 0.0332$ (Blichert-Toft and Albarède 1997) were used for the calculation of εHf(t) values. Model ages (T_{DM}, T_{DM}^c) were calculated by the current $^{176}Hf/^{177}Hf = 0.28325$ and $^{176}Lu/^{177}Hf = 0.0384$ of depleted mantle (Griffin et al. 2000) and the average continental ratios of $^{176}Lu/^{177}Hf = 0.015$ reported by Griffin et al. (2002).

Results

Samples from Hadahushu group

Sample 20ZH23: Zircons from this sample are generally euhedral and prismatic in shape with oscillatory zones (Fig. 7A), indicating a magmatic origin. Ninety zircons were randomly selected for U–Pb dating, and 65 grains of them have concordant ages (Fig. 8A, B; Table S1). The Th/U ratios of these zircons range from 0.17 to 2.32 except for two grains (0.04 and 0.07). Approximately one third of the concordant ages are early Paleozoic ranging from ~ 421 to ~ 524 Ma with a prominent peak at 446 Ma. Precambrian zircon ages can be fall into five populations: 591–934 Ma (peak ages at 586 Ma and 910 Ma), 1010–1360 Ma (peak at 1243 Ma), 1423–1650 Ma (peak at 1465 Ma), 1714–2234 Ma (peak at 1825 Ma), and another two grains have Archean ages of 2524 Ma and 2732 Ma.

Twenty grains with concordant ages were analyzed for Lu–Hf isotopic compositions (Fig. 10; Table S2). The εHf(t) values of early Paleozoic zircons range from -23.9 to + 5.9, with the two-stage Hf model ages (T_{DM}^c) ranging from 1036 to 2923 Ma. The Neoproterozoic to Paleoproterozoic zircons yield mostly positive εHf(t) values from 0.7 to + 13.4, and only four of them have negative εHf(t) values from − 1.7 to − 12.2.

Sample 20ZH24: zircons from this sample have sub-rounded to prismatic shape with clear oscillatory zones and their length–width ratios ranging from 1:1 to 3:1 (Fig. 7B). Ninety zircons were selected randomly for U–Pb isotopic analyses of which 83 grains yield concordant ages from 418 to 2882 Ma (Fig. 8C, D; Table S1). Their Th/U ratios vary from 0.16 to 1.26 except one zircon of 0.09. Twenty-eight (30%) of them are early Paleozoic ages from 418 to 532 Ma with a prominent peak at 445 Ma. Two youngest zircons have ages of 418 ± 4 Ma and 421 ± 4 Ma. Precambrian zircons are grouped as: 563–608 Ma (peak at 580 Ma), 833–1673 Ma (peak at 1068 Ma), 1730–1944 Ma (peak at 1765 Ma), 2233–2467 Ma, and 2560–2882 Ma.

Lu–Hf isotopic analyses were performed on twenty-three zircons with concordant ages (Fig. 10; Table S2). Most early Paleozoic zircon grains (~ 70%) yield negative εHf(t) values from -30.3 to -6.4, and two grains have positive εHf(t) values of + 3.7 and + 3.4. The T_{DM}^c model ages of these early Paleozoic grains range from 1180 to 3327 Ma. The Precambrian zircons are also dominated by negative εHf(t) values from

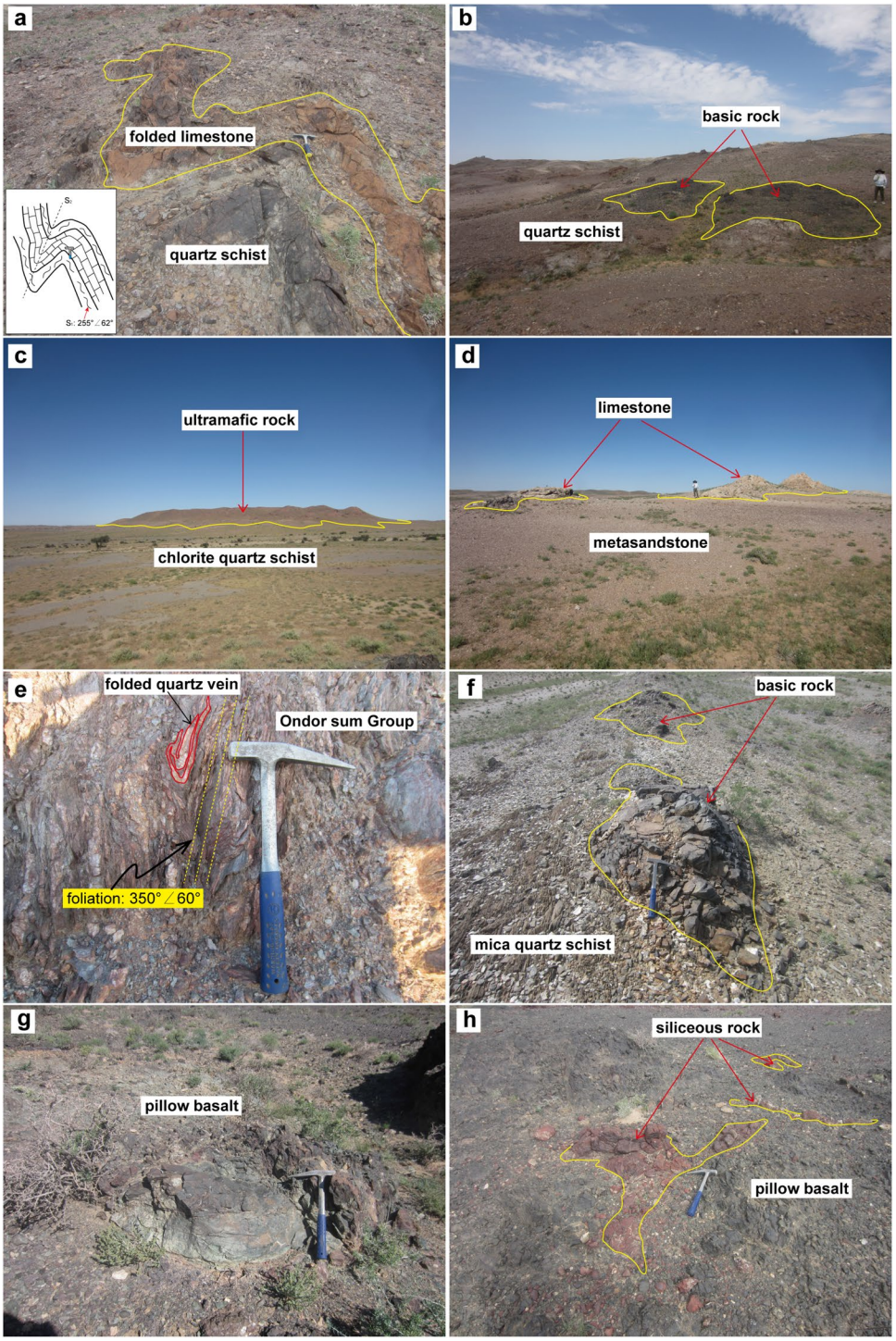

Fig. 6 Field characteristics of ophiolitic mélange within the early Paleozoic strata in the Ganqimaodu area. **a** limestone block within quartz schist and folded together; **b** blocks of the basic rocks in quartz schist; **c** block of carbonatation ultramafic rock in chlorite–quartz schist; **d** limestones as blocks within metasandstone matrix; **e** intense deformed strata of the Ondor sum Group, quartz veins developed along the foliation and folded; **f** block-in-matrix structure: basic rocks as the blocks and mica quartz schist as the matrix; **g** pillow basalt within the strata of the Ondor sum Group; **h** red siliceous rocks encased within pillow basalt. The locations of all field photographs are shown in Fig. 3

− 44.7 to − 1.0 except for three grains with εHf(t) values from + 0.2 to + 5.9. More than half of Precambrian zircons have Archean T_{DM}^{c} model ages.

Sample 20ZH16: Most zircon grains show clear oscillatory zones with subrounded to prismatic shapes (Fig. 7C). Ninety grains were analyzed of which 84 grains yield concordant ages (Fig. 8E, F; Table S1). Except two spot of 0.06 and 0.07, their Th/U ratios range from 0.15 to 2.89. Paleozoic zircons occupy 17.9% with ages from 427 to 523 Ma with a prominent age peak at 470 Ma. Precambrian zircons are abundant in this sample and are grouped as: 573–998 Ma (peak at 953 Ma), 1064–1368 Ma (peak at 1112 Ma), 1410–2059 Ma (peak ages at 1458 Ma, 1761 Ma, and 1986 Ma), 2286–2497 Ma (peak at 2380 Ma), and three grains yield Archean ages of 2721 Ma, 2802 Ma and 3079 Ma.

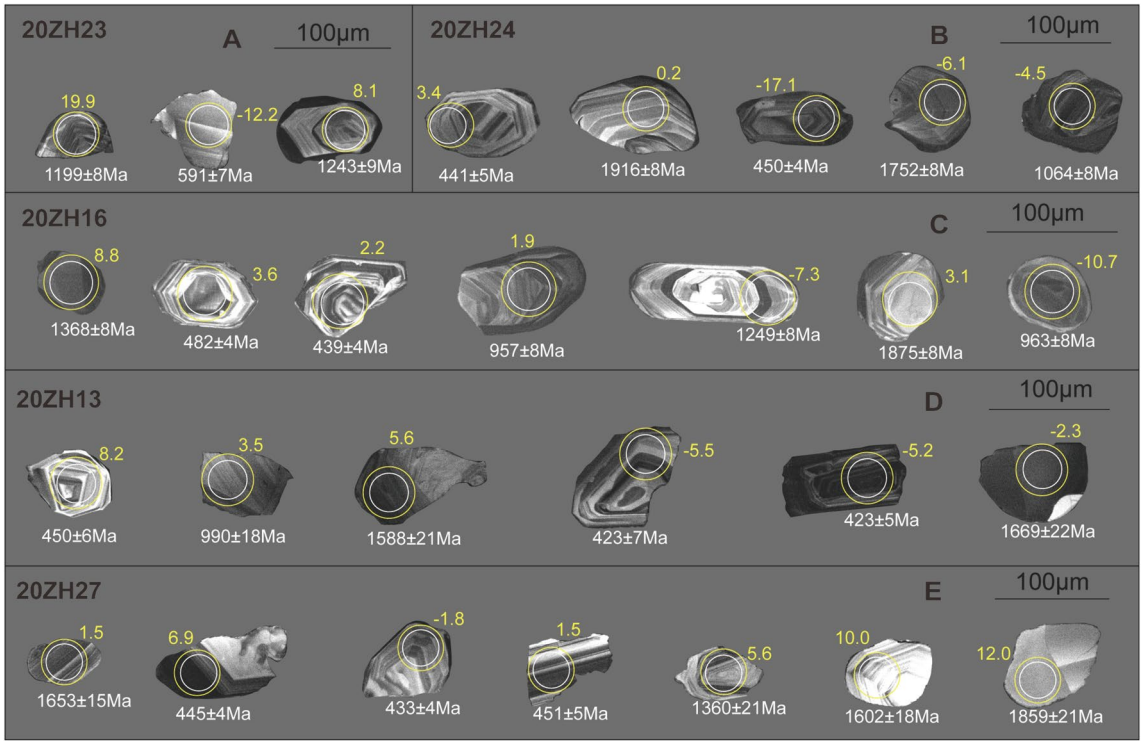

Fig. 7 Cathodoluminescence (CL) images for representative zircons from samples in this study. The white and yellow circles are analysis situs of U–Pb and Lu–Hf isotope, respectively. The white numbers are U–Pb ages with 2σ uncertainty, and the yellow numbers are εHf(t) values

Lu–Hf isotopic compositions were analyzed for twenty-eight zircon grains with concordant ages (Fig. 10; Table S2). Early Paleozoic zircons yield mostly positive εHf(t) values from + 1.9 to + 5.8, and one grain with εHf(t) value of -7.0. These early Paleozoic grains have T_{DM}^{c} ages ranging from 1085 to 1895 Ma. The Precambrian zircons have εHf(t) value of − 10.7 ~ + 8.8. The T_{DM}^{c} ages of Precambrian zircon grains range from 1275 to 4000 Ma and two grains have Archean model ages.

Samples from Ondor sum group

Sample 20ZH13: Almost all zircons from this sample are euhedral and prismatic with clear oscillatory zones (Fig. 7D), indicating a proximal magmatic source. Ninety zircons were analyzed for U–Pb isotopes of which 78 grains yield concordant ages with Th/U ratios of 0.12–2.55. (Fig. 8G, H; Table S1). About 42% of them are Paleozoic ages from 404 to 524 Ma with a peak at 423 Ma, in accordance with a weighted mean age of 421 ± 3 Ma of fifteen clustered ages of Paleozoic grains. The youngest grain yielded an age of 404 ± 7 Ma. Precambrian zircons are grouped as 573–1493 Ma (peaks at 615 Ma and 1172 Ma) and 1525–2058 Ma (peak at 1588 Ma), and the remaining two grains have ages of 2440 Ma and 2646 Ma.

Lu–Hf isotopic analyses were performed on 27 zircon grains with concordant ages (Fig. 10; Table S2). The εHf(t) values of early Paleozoic zircons range from -5.5 to + 9.1, and T_{DM}^{c} ages of them range from 849 to 1751 Ma. Zircons with Mesoproterozoic to Paleoproterozoic ages have εHf(t) values from − 6.0 to + 7.2 with T_{DM}^{c} ages from 1493 to 3203 Ma.

Sample 20ZH27: Most zircons from this sample are euhedral and prismatic with clear oscillatory zones (Fig. 7E). Ninety zircon grains were randomly selected for U–Pb dating and 68 of them yield concordant ages (Fig. 8I, J; Table S1). All analysis spots have Th/U ratios from 0.12 to 1.59. About 1/3 are Paleozoic ages from 415 to 523 Ma with a peak at 441 Ma. The ages of Precambrian zircons range from 543 to 2753 Ma, which yield four major peaks at 959 Ma, 1600 Ma, 1950 Ma and 2564 Ma.

Twenty-seven zircon grains with concordant ages were analyzed for Lu–Hf isotopic compositions (Fig. 10; Table S2). These early Paleozoic zircons have mostly positive εHf(t) values from 0.0 to + 6.9, and three grains exhibit negative εHf(t) values from − 1.8 to − 3.4. The two-stage Hf model ages (T_{DM}^{c}) of these early Paleozoic zircon grains range from 982 to 1639 Ma. Two Neoproterozoic grains have negative εHf(t) values of − 6.9 and − 11.9. Zircons with Paleoproterozoic to Archean ages yield almost all positive εHf(t) values except for a εHf(t) value of − 1.7. Precambrian

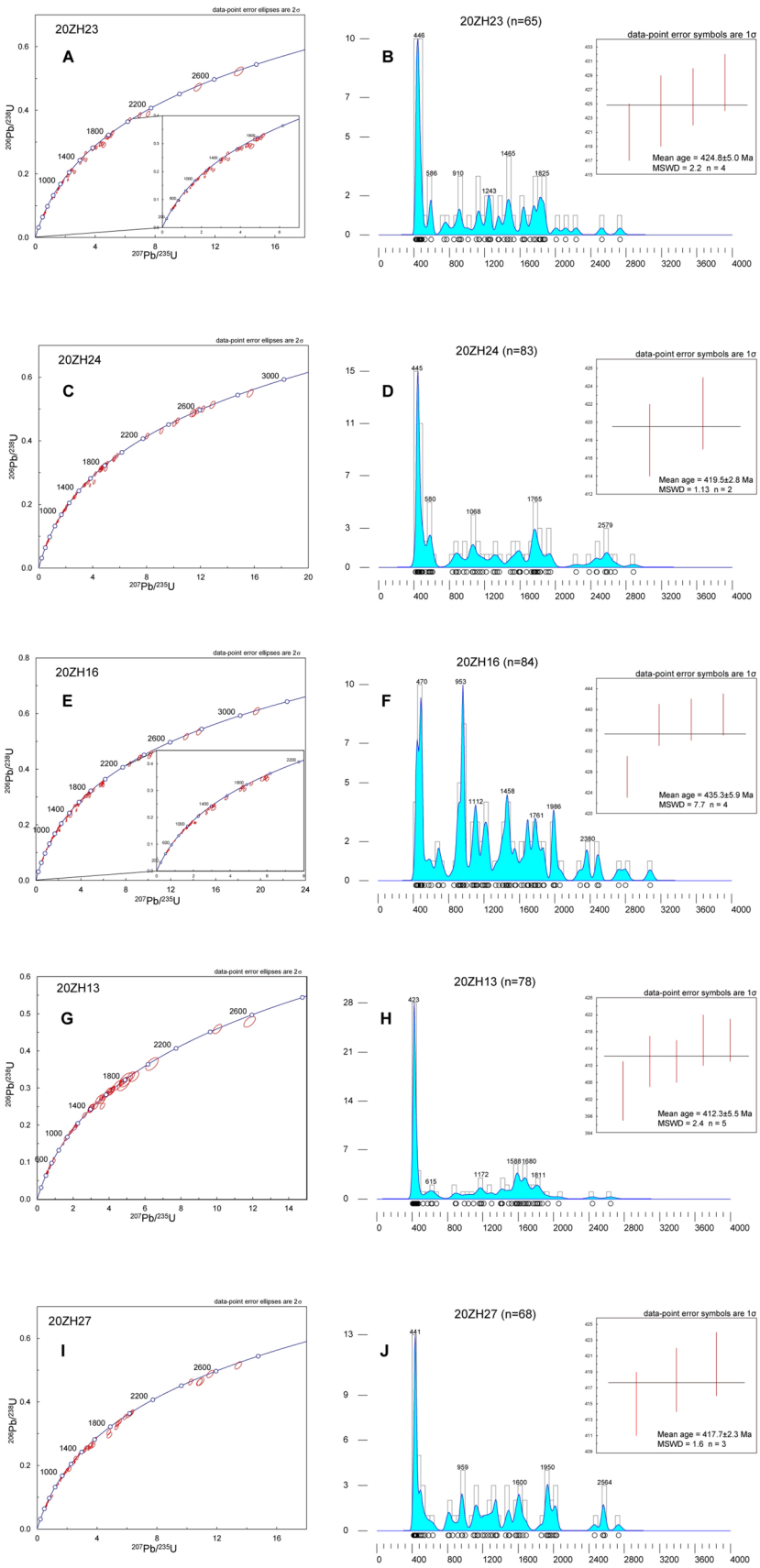

Fig. 8 U–Pb concordia diagrams and Kernel Density Estimate (KDE) for detrital zircons from the (meta)sedimentary rocks in this study

grains have T_{DM}^{c} ages ranging from 1480 to 3018 Ma, of which four zircons have Archean model ages.

Discussion

Constraints on depositional ages

The maximum depositional age (MDA) of a sedimentary unit can be assessed by the youngest detrital zircon age, and it could be closed to the real depositional age in some situations (Dickinson and Gehrels 2009; Gehrels 2014). According to Dickinson and Gehrels (2009), the youngest detrital zircon age of a sedimentary rock can be measured by diverse ways such as: the youngest single detrital grain age (YSG), the weighted mean age of youngest cluster of two or more zircon ages overlapping at 1σ uncertainty (YC1σ (2+)), or the youngest graphical detrital zircon age peak (YPP). In this paper, we regard the YC1σ (2+) as the MDAs for all samples, and the YSG and YPP are considered as the reference data for the MDAs (Fig. 8; Table 1).

Due to a lack of biostratigraphic data, the age of the Ondor sum Group strata in the study area was roughly estimated to Neoproterozoic based on metamorphic grade and regional geological correlations (Anonymous 1980a). However, the depositional age of the Ondor sum Group in the Tulinkai area to the east of the study area was constrained as Cambrian to Middle Silurian (Li et al. 2012). Xu et al. (2016) suggested that the Ondor sum Group from the western Inner Mongolia was mainly deposited in the early Paleozoic based on stratigraphic correlation. Two chlorite–quartz schists (samples 20ZH13 and 20ZH27) from the Ondor sum Group in the study area yield MDAs of 412.3 ± 5.5 Ma and 417.7 ± 2.3 Ma, respectively (Table 1), which constrain the strata to early Devonian.

The coral fossils including *Petraea sp.*, *Orthophyllum sp.* and *Propora sp.* from limestone blocks within the lower part of the Hadahushu Group strata were reported, and their ages are constrained to early–middle Silurian (Anonymous 1980a, b). Moreover, Tian et al. (2019e) also suggested that the Hadahushu Group formed in the early–middle Silurian based on detrital zircon ages. In this study, a meta-quartz sandstone (sample 20ZH16) has a MDA of 435.3 ± 5.9 Ma calculated by a weighted mean age of four youngest grains overlapping at 1σ uncertainty. Another two quartz sandstones (samples 20ZH23 and 20ZH24) have MDAs of 424.8 ± 5.0 Ma and 419.5 ± 2.8 Ma (Table 1). Our new data indicate that the depositional age of the Hadahushu Group should be later than late Silurian. Field relationship shows that the Hadahushu Group unconformably overlies the Ondor sum Group in the Ganqimaodu area. Therefore, we suggest that the Hadahushu Group was also deposited in early Devonian.

Provenance analyses

All samples from the Ondor sum Group and the Hadahushu Group have similar detrital zircon age patterns which contain prominent early Paleozoic ages with extensive Precambrian ages (Fig. 8). The early Paleozoic grains were likely derived from nearby subduction-related plutons consisting of quartz diorites and granitoids in the Ganqimaodu area (Xu et al. 2013; Zhang et al. 2019b; our unpublished data; Fig. 3). This is also consistent with the shapes of the zircon grains which are euhedral and prismatic with distinct oscillatory zones (Fig. 7). Precambrian zircons of the Hadahushu Group occupy a greater proportion than those of the Ondor sum Group (Fig. 8). It may suggest that more input of exposed Precambrian basement with continuous consumption of the early Paleozoic plutons. Sample 20ZH16 from the Hadahushu Group has a great deal of Precambrian zircons (about 82%) with a prominent Neoproterozoic peak (~ 953 Ma). The detrital zircon age spectrums of samples 20ZH23 and 20ZH24 are very similar, whose Precambrian zircons take an amount of about 70%. For the Ondor sum Group strata, early Paleozoic zircons of sample 20ZH13 have a larger proportion than those of sample 20ZH27. Precambrian zircons of sample 20ZH13 have a prominent peak at 1588–1680 Ma, while those of sample 20ZH27 are relatively scattered

Table 1 Detrital zircon ages and maximum depositional age constraints for these (meta)sedimentary rocks from the study area

Sample no.	Stratigraphic units	Detrital zircon U–Pb ages		Maximum depositional ages (MDA)		
		Concordant analyses	Age ranges/Ma	YSG (1σ)/Ma	YC1σ (2+)/Ma	YPP/Ma
20ZH23	Hadahushu group	65	421–2732	421 ± 4	424.8 ± 5.0 (MSWD = 2.2, *n* = 4)	446
20ZH24	Hadahushu group	83	418–2882	418 ± 4	419.5 ± 2.8 (MSWD = 1.13, *n* = 2)	445
20ZH16	Hadahushu group	84	427–3079	427 ± 4	435.3 ± 5.9 (MSWD = 7.7, *n* = 4)	470
20ZH13	Ondor sum group	78	404–2646	404 ± 7	412.3 ± 5.5 (MSWD = 2.4, *n* = 5)	423
20ZH27	Ondor sum group	68	415–2735	415 ± 4	417.7 ± 2.3 (MSWD = 1.6, *n* = 3)	441

YSG, Youngest single detrital zircon age; *YC1σ (2+)*, Weighted mean age of youngest cluster of two or more zircon ages overlapping at 1σ uncertainty; *YPP* youngest detrital zircon age peak

with a few minor peaks at ~ 959 Ma, ~ 1600 Ma, ~ 1950 Ma and ~ 2564 Ma (Fig. 8H, J). All detrital zircon ages from the Ondor sum Group and Hadahushu Group in this study are pooled together respectively. The Ondor sum Group has age peaks at ~ 425, ~ 966, ~ 1590, ~ 1930 and ~ 2564 Ma, while the Hadahushu Group yields a series of peaks at ~ 443, ~ 586, ~ 960, ~ 1473, ~ 1765 and ~ 2480 Ma (Fig. 9). These two sets of strata display similar detrital zircon age spectrums with some slight differences between early Mesoproterozoic and late Paleoproterozoic. Based on the above comparison for the detrital zircon ages, we suggest that sediments of these two sets of strata are much more likely from the same source.

When pooling all the data from early Devonian strata in the Ganqimaodu area together, they yield a prominent early Paleozoic peak at ~ 452 Ma and subordinate Precambrian age peaks at ~ 587 Ma, ~ 961 Ma, ~ 1120 Ma, ~ 1482 Ma, ~ 1761 Ma, and ~ 2560 Ma (Fig. 11C). To the east of the study area, the Bainaimiao Arc, has a very similar detrital zircon spectrum with early Devonian strata from the Ganqimaodu area (Fig. 11B; age peaks at ~ 457 Ma, ~ 578 Ma, ~ 975 Ma, ~ 1103 Ma, ~ 1567 Ma, ~ 1864 Ma, and ~ 2478 Ma). A lot

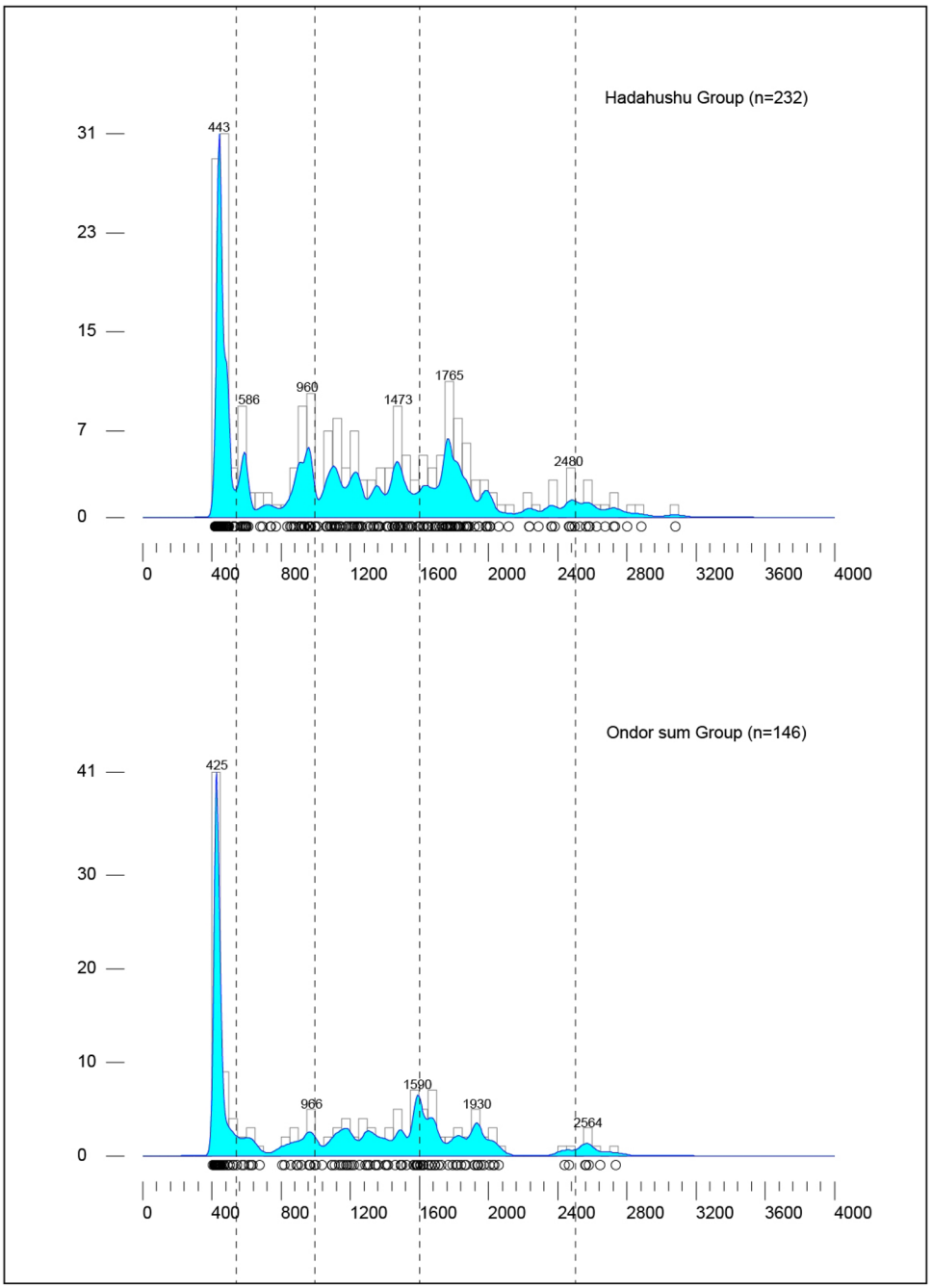

Fig. 9 Comparison of detrital zircon populations from the Ondor sum Group and Hadahushu Group in the study area

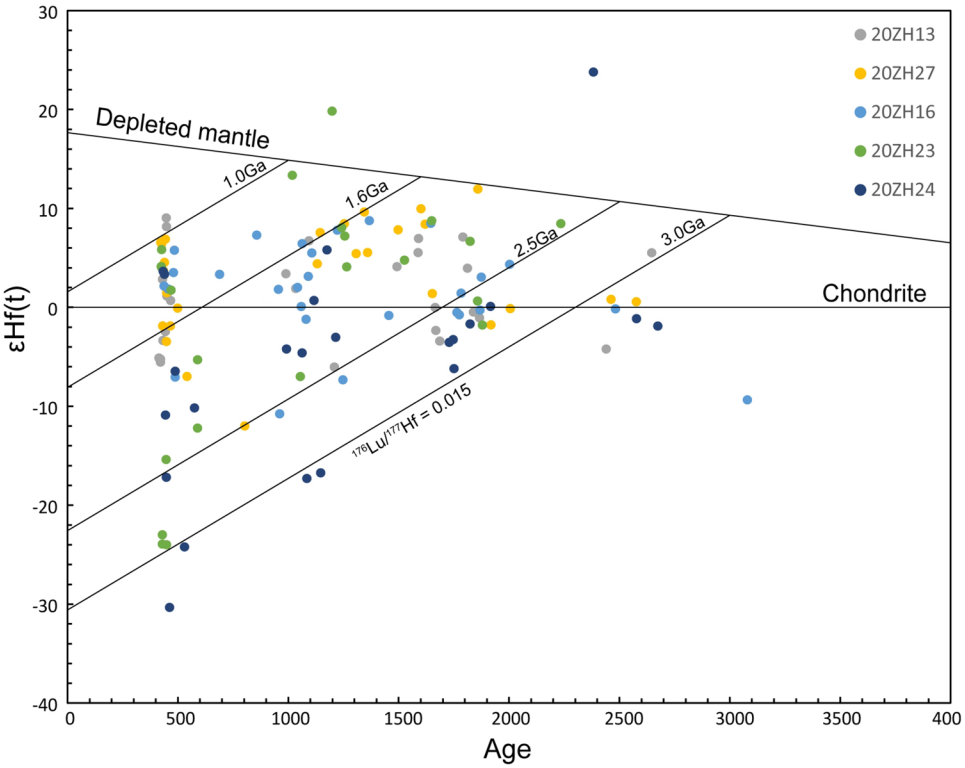

Fig. 10 The diagram of Zircon U–Pb age versus εHf(t) of the early to middle Paleozoic sedimentary rocks in the study area

of early Paleozoic (ca. 420–500 Ma) arc-related igneous rocks with both positive and negative εHf(t) values (−9.3 to 11.4) developed in the Bainaimiao Arc, indicating juvenile crust growth and ancient crust reworking (Chen et al. 2020; Zhang et al. 2014; Zhou et al. 2018b). This is consistent with early Paleozoic detrital zircons from early Devonian strata in the study area which also have both positive and negative εHf(t) values (Figs. 10 and 12B). It seems to indicate that not only these intrusions from the Ganqimaodu area but also magmatic rocks from the Bainaimiao Arc have been the main source for these early Paleozoic detrital zircons from the early Devonian strata. There are distinct changes for εHf(t) values of Mesoproterozoic to Late Paleoproterozoic zircons from the early Devonian strata in the Ganqimaodu area: an increasing εHf(t) values of zircons from late Paleoproterozoic to middle Mesoproterozoic with a decreasing εHf(t) values of zircons from middle Mesoproterozoic to late Mesoproterozoic. These changes are also consistent with εHf(t) values of contemporaneous zircons from the Bainaimiao Arc (Fig. 12B). Our results show that the Ganqimaodu area may represent the western part of the Bainiamiao Arc, where the early Paleozoic arc-related magmatic rocks and Proterozoic basement were the main sources for these early Devonian strata in the study area. Recently, the Bainaimiao Arc was suggested as an exotic block with respect to the North China Craton and has a tectonic affinity to the Tarim Craton based on detrital zircon ages and Hf isotopes comparison (Zhang et al. 2014; Zhou et al. 2020; Fig. 11F and Fig. 12A). Plenty of ~ 889–980 Ma Neoproterozoic granitoids or granitic gneisses were reported in the Southern Mongolian accretionary system to the north of the study area (Demoux et al. 2009; Wang et al. 2001; Zhang et al. 2017b; Zhou et al. 2013b; Fig. 11A), which may provide detritus to the early Devonian sedimentary rocks in the Ganqimaodu area. The sediments of the early to middle Paleozoic strata from the north Alxa (Zhusileng–Hangwula Tectonic Zone) were also considered to be derived from the northern microcontinent of the CAOB such as Central Tianshan, South Beishan or South Mongolia (Chen et al. 2019; Yin et al. 2015; Fig. 11E).

A few detrital zircon age peaks of the Nuru–Langshan Tectonic Zone are also similar to those of early Devonian strata from the Ganqimaodu area (Fig. 11C, D). However, it is largely excluded as the source by comprehensive analysis for our data, based on following reasons. First, although the early Paleozoic magmatic rocks also developed in the Nuru–Langshan Tectonic Zone, almost all magmatic zircons from these rocks have negative εHf(t) values (Dan et al. 2016; Liu et al. 2016b; Teng et al. 2019; Tian et al. 2019a; Fig. 12C). They are different from early Paleozoic detrital zircons of these early Devonian (meta)sedimentary rocks from the Ganqimaodu area which have both positive and negative εHf(t) values (Fig. 10). Second, Neoproterozoic magmatic events from the Nuru–Langshan Tectonic Zone occurred mainly between ~ 800 Ma and ~ 930 Ma, represented by ~ 805 Ma and ~ 817 Ma acid volcanic rocks

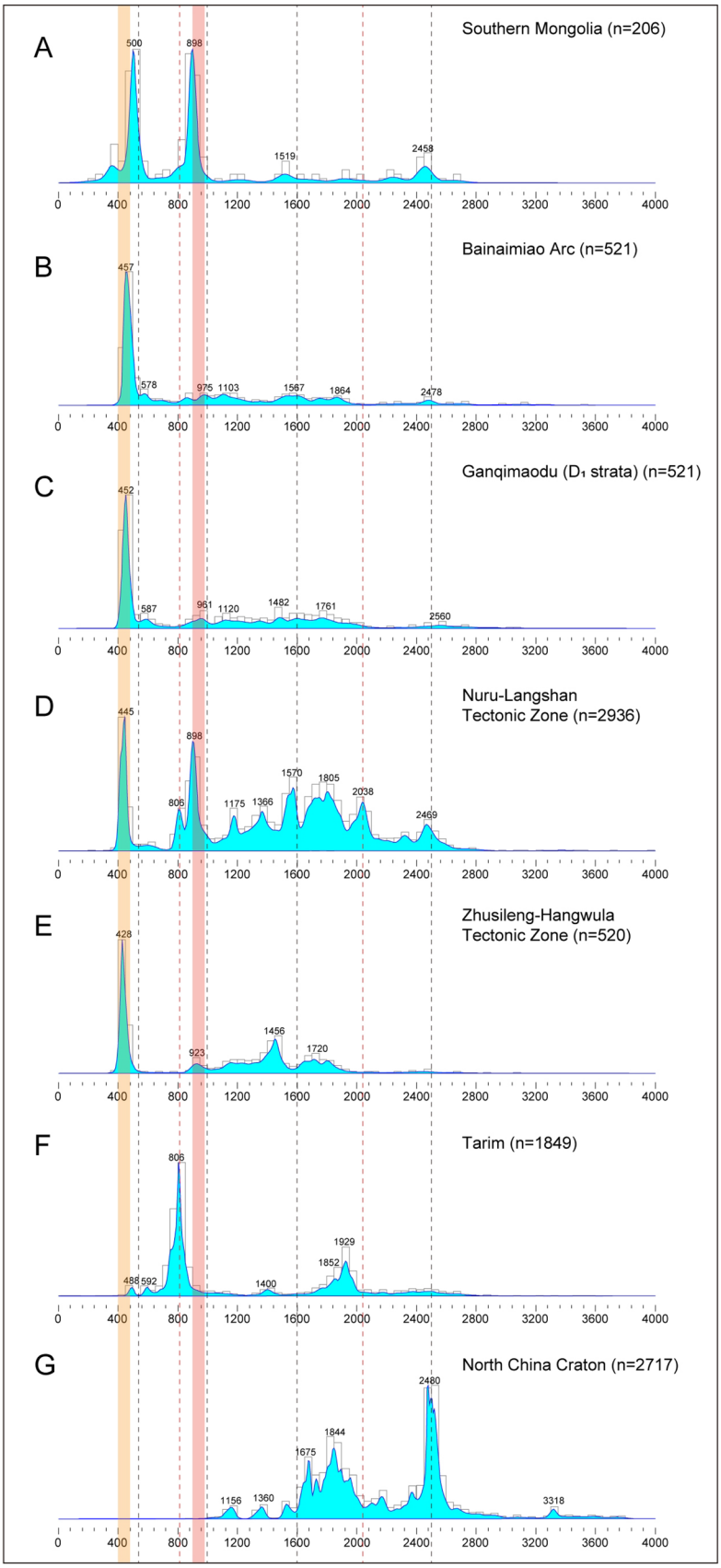

Fig. 11 Comparison of the age populations of the zircons from: **A** Southern Mongolia (Demoux et al. 2009; Rojas-Agramonte et al. 2011; Wang et al. 2001; Zhang et al. 2016b; Zhou et al. 2013a); **B** Bainaimiao Arc (Chen et al. 2020; Zhang et al. 2014, 2017a; Zhou et al. 2020); **C** Early Devonian strata of the Ganqimaodu area (Tian et al. 2019e; this study); **D** Nuru–Langshan Tectonic Zone (Bao et al. 2019; Dan et al. 2012, 2014b, 2016; Geng and Zhou 2010; Gong et al. 2016; Hu et al. 2014; Liu et al. 2019a, 2016b; Peng et al. 2010; Song et al. 2017; Sun et al. 2013; Teng et al. 2019; Tian et al. 2019c; Wang et al. 2015b, 2016b; Xiao et al. 2015b; Zhang et al. 2013a); **E** Zhusileng–Hangwula Tectonic Zone (Chen et al. 2019; Yin 2016; Yin et al. 2015); **F** Tarim Craton (Rojas-Agramonte et al. 2011; Zhu et al. 2021); **G** North China Craton (Liu et al. 2017a; Rojas-Agramonte et al. 2011; Wang et al. 2015a; Zhou et al. 2020)

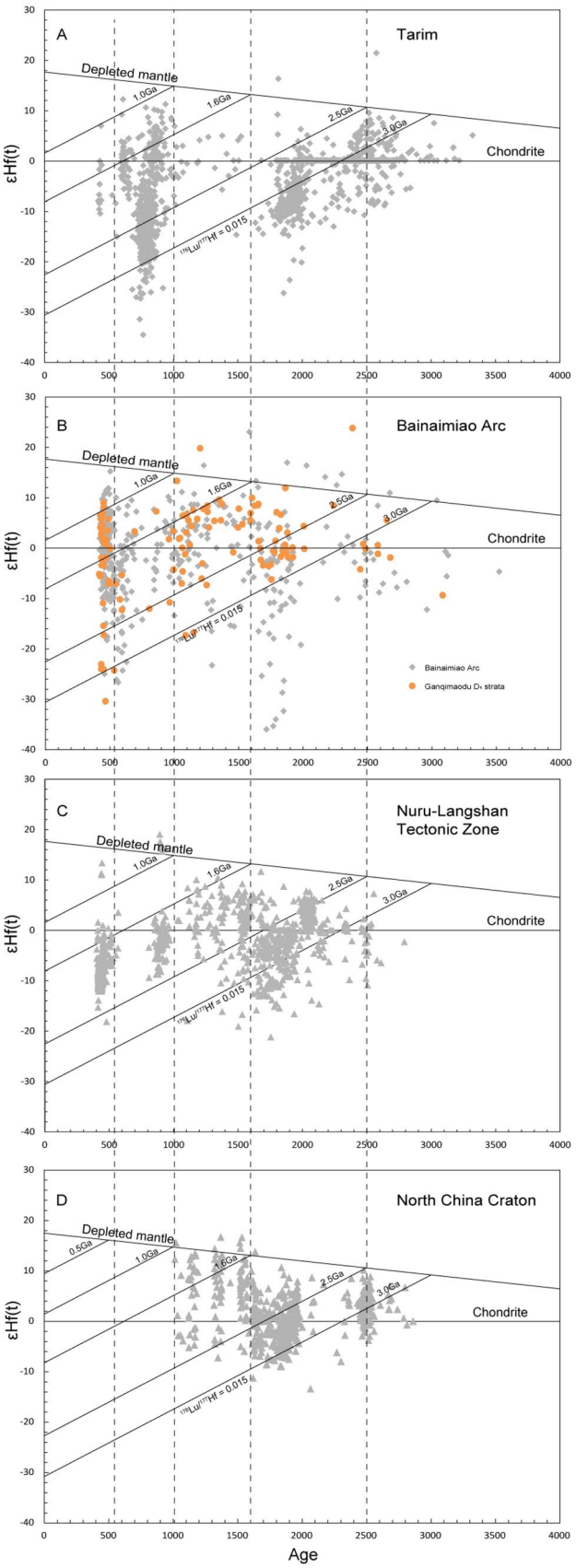

Fig. 12 Comparison of U–Pb age versus εHf(t) for Early Devonian (meta)sedimentary rocks in the Ganqimaodu area with adjacent tectonic units and cratons. Date sources: **A** Tarim Craton (He et al. 2014a, 2014b; Li et al. 2015; Zheng et al. 2020); **B** Bainaimiao Arc (Chen et al. 2020; Wang et al. 2016a; Zhang et al. 2014; Zhou et al. 2018a, 2020) and Early Devonian strata of the Ganqimaodu area (this study); **C** Nuru–Langshan Tectonic Zone (Bao et al. 2019; Dan et al. 2012, 2014b, 2016; Gong et al. 2016; Liu et al. 2016b, 2019a; Teng et al. 2019; Tian et al. 2019c); **D** North China Craton (Liu et al. 2017a; Wang et al. 2015a; Zhou et al. 2020)

from the Langshan area (Peng et al. 2010), and ~ 910 Ma and ~ 930 Ma granite plutons from the Bayinnuoergong area (Dan et al. 2014b). However, these magmatic zircons are lacking in early Devonian sedimentary rocks from the Ganqimaodu area. The prominent Neoproterozoic age peaks (~ 587 Ma, ~ 961 Ma) of these early Devonian strata in the study area are inconsistent with those (peaks at ~ 806 Ma, ~ 898 Ma) of the Nuru–Langshan Tectonic Zone (Fig. 11C, D). Third, abundant late Mesoproterozoic (Stenian) zircons with both positive and negative εHf(t) values are detected from the Ganqimaodu early Devonian sediments, whereas contemporaneous zircons from the Nuru–Langshan Tectonic Zone are relatively few and almost all of them have positive εHf(t) values (Fig. 12B, C). Besides, a significant Paleoproterozoic age peak of the Nuru–Langshan Tectonic Zone is at ~ 2038 Ma, which is also absent in the early Devonian strata from the study area (Fig. 11C, D). The εHf(t) values of Mesoproterozoic to middle Paleoproterozoic zircons from the Nuru–Langshan Tectonic Zone have an increasing tendency with decreasing age, similar to the evolutionary trend of those of the North China Craton (Fig. 12C, D). However, it is different from the variation trend of εHf(t) values of Mesoproterozoic to middle Paleoproterozoic zircons from the Ganqimaodu area and the Bainaimiao Arc (Fig. 12B). In addition, the North China Craton is excluded as source for these early Devonian strata in the study area based on the missing of early Paleozoic to Neoproterozoic magmatic events (Fig. 11G).

In summary, through comparison of the detrital zircon ages and Hf isotopes from the study area and the adjacent tectonic units, we suggest that early Devonian strata from the Ganqimaodu area are the western extension of the Bainaimiao Arc. Early Paleozoic magmatic rocks and Precambrian basement of the Bainaimiao Arc are the main sources for these strata. Also, the Southern Mongolia to the north of the study area is a significant source for them. However, to the south of the Ganqimaodu area, the Nuru–Langshan Tectonic Zone cannot provide detritus for these strata in the study area. Field investigations show that early Devonian strata from the study area are in fault contact with Mesoproterozoic strata from the Nuru–Langshan Tectonic Zone (our unpublished data; Figs. 3 and 4). Thus there might exist a barrier (may be an ocean) to impede the transportation for

the materials from the the Nuru–Langshan Tectonic Zone during early Devonian. The South Bainaimiao ocean proposed by Zhang et al. (2014) between the Bainaimiao Arc and the North China Craton may extend to here westward, and consumption of the ocean basin leads to the final collision between the Ganqimaodu area (the western part of the Bainaimiao Arc) and the Nuru–Langshan Tectonic Zone.

Tectonic setting

The detrital zircon age spectra may reflect the tectonic setting of sedimentary basins (Cawood et al. 2012). Based on the age distribution patterns from different types of basins all over the world, Cawood et al. (2012) proposed that the tectonic setting of sedimentary rocks can be distinguished through plotting cumulative proportion curves of the difference values between the crystallization ages (CA) and the depositional age (DA). The sediments that CA–DA smaller than 100 Ma at the youngest 30% belong to convergent setting; while sediments from the collisional setting have CA–DA smaller than 150 Ma at the youngest 5% and greater than 100 Ma at the youngest 30%; others are extensional setting (Fig. 13). All samples in this study are plotted in the Fig. 13, and the depositional ages were defined by the MDAs of these (meta)sedimentary rocks as mentioned above.

Almost all samples from the early Devonian strata in this study except for sample 20ZH16 fall into the convergent setting. Two sedimentary rocks from the Hadahushu Group reported by Tian et al. (2019e) also fall into the convergent setting. The results are also consistent with existence of nearby subduction-related diorites with depletions in Nb, Ta in the Ganqimaodu area (Xu et al. 2013; Zhang et al. 2019b; our unpublished data; Fig. 3). Moreover, according to Anonymous (1980a, b), there may be blueschist in the southern part of the study area, which formed in subduction zone setting. This is conflicted with the passive margin deposition and foreland basin deposits proposed by Xu et al. (2013). In addition, provenance analyses of these (meta) sedimentary rocks also indicate that sediments are mainly from a northern unidirectional provenance. It is different from the back-arc basin setting which generally has bidirectional provenance. Ophiolitic mélanges containing blocks of ultramafic–mafic rocks, pillow basalts, siliceous rocks, and carbonate rocks are widespread in the early Devonian strata from the Ganqimaodu area (Fig. 6). The Ondor sum Group, which is considered as matrix of ophiolitic mélanges, has undergone greenschist-facies metamorphism with multiphase structural deformations. A few basic rocks blocks within the Ondor sum Group have also undergone metamorphism of amphibolite facies (our unpublished data; Fig. 6). The lower part of Hadahushu Group is mainly characterized by a set of thick flysch deposition composed of unmetamorphosed sandstone, siltstone and mudstone (Fig. 5), which may represent a trench-slope basin deposition above deformed accretionary prism (the Ondor sum Group). Therefore, we advocate that the early Devonian (meta)sedimentary rocks in the Ganqimaodu area form parts of an accretionary complex.

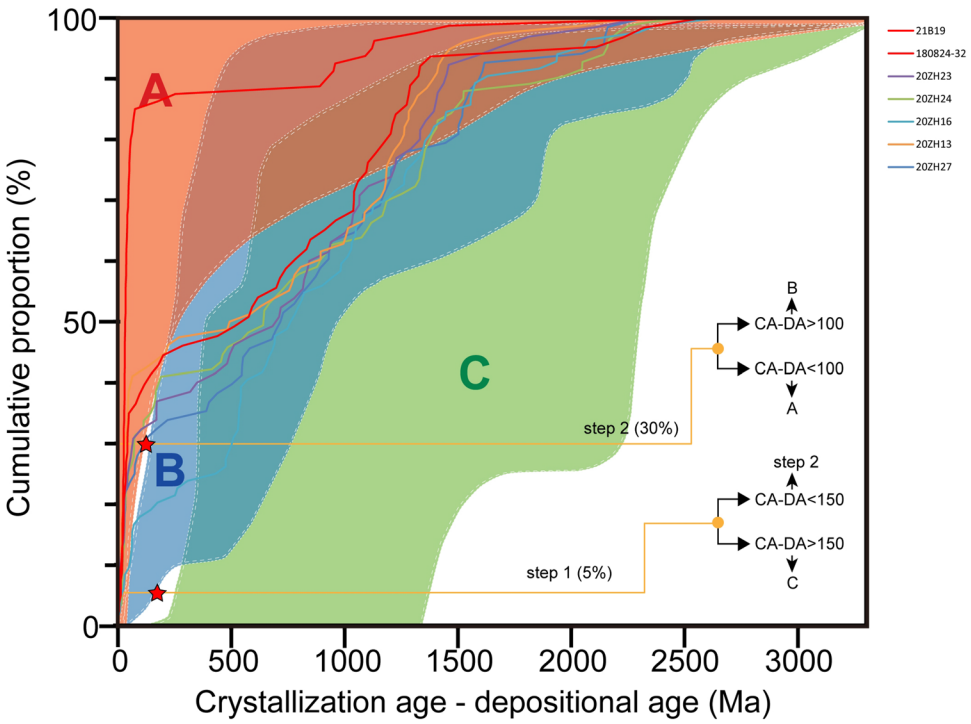

Fig. 13 Cumulative proportion curves of the difference values between the crystallization ages and the depositional age of the (meta)sedimentary rocks from the Ganqimaodu area. Samples 21B19 and 180,824–32 are from Tian et al. (2019e) and other samples are from this study. **A** Convergent setting, **B** Collisional setting, **C** Extensional setting. Modified after Cawood et al. (2012)

Early Paleozoic subduction polarity: southward or northward

Controversy remains for early Paleozoic subduction polarity of the PAO along the Alxa Tectonic Belt and the Bainaimiao Arc. Most authors favor a southward subduction of the PAO in the east segment of the southern CAOB. The early Paleozoic Ondor sum accretionary complexes were suggested as the products of the southward subduction of the PAO beneath the North China Craton (Xiao et al. 2003). The Tulinkai SSZ ophiolites to the south of the Ondor sum area were also considered to be related to southward subduction of the PAO during early Paleozoic (Jian et al. 2008). In addition, Liu et al. (2016b) also proposed the southward subduction of the PAO along the Alxa Tectonic Belt and the northern North China Craton based on comparable arc-related plutons.

However, the Bainaimiao Arc has been suggested as an exotic block relative to North China Craton and a northward subduction of the South Bainaimiao Ocean in the Early Paleozoic was proposed to explain the origin of the Bainaimiao Arc (Zhang et al. 2014). The existence of the South Bainaimiao Ocean is evidenced by a series of early Paleozoic ophiolitic mélanges along the north margin of the North China Craton: the Xiaowulanhua mélange (Liu et al. 2020), the Chegandalai mélange (Hu 2019), the Hongqi mélange (Shi et al. 2013), the Wude mélange (Jia et al. 2003; Shang et al. 2003), and the Ganqimaodu mélange (Xu et al. 2013; Fig. 3 and Fig. 6). Moreover, the northward subduction of the South Bainaimiao Ocean is largely supported by the early Paleozoic passive continental margin for the northern North China Craton which has a widely distributional epicontinental sea deposition without magmatic events (Chen et al. 2015; Zhang et al. 2014; Zhao et al. 2017).

Field data and provenance analyses of (meta)sedimentary rocks from this study show that early Devonian strata in the Ganqimaodu area were parts of an accretionary wedge along the south flank of the Bainaimiao Arc, which support the northward subduction of the South Bainaimiao Ocean. Moreover, our data also imply that the western segment of the South Bainaimiao Ocean must be wide enough so that detritus from the Nuru–Langshan Tectonic Zone cannot be transported to the Ganqimaodu area during early Devonian. Previously the Hadahushu Group from the study area was considered as the western extension of the Xuniwusu Formation in the Bainaimiao area to the east of the study area (Tian et al. 2019e; Xu et al. 2013). Detailed studies for the early Silurian Xuniwusu Formation showed that the Bainaimiao Arc provided almost all detritus for the lower part, while the detritus of the upper part was not only derived from the Bainaimiao Arc but also from the North China Craton (Zhang et al. 2017a). The variation of provenance of the Xuniwusu Formation seems to indicate that the North China Craton were close to the Bainaimiao Arc gradually until they collided with each other. Different from the previous opinion proposed by Zhang et al. (2017a) that the Xuniwusu Formation was an early Paleozoic back-arc basin deposit above the North China Craton, we suggest that the Xuniwusu Formation could be the forearc deposition by the northward subduction of the South Bainaimiao Ocean and was in contact with the passive margin of the northern North China Craton subsequently. Silurian intrusions from the northern Alxa area also indicate that the South Bainaimiao Ocean subducted beneath the Southern Mongolia to the north during early Paleozoic (Zheng et al. 2016). Therefore, it is clear that the northward subduction of the South Bainaimiao Ocean is widespread along the Bainaimiao Arc and the Southern Mongolia.

To the south of the South Bainaimiao Ocean, the Nuru–Langshan Tectonic Zone was active continental margin evidenced by early Paleozoic arc-related magmatism (Dan et al. 2016; Liu et al. 2016b; Teng et al. 2019; Tian et al. 2019a). Liu et al. (2016b) argued that early Paleozoic magmatic events from the Nuru–Langshan Tectonic Zone and the Bainaimiao Arc are comparable based on rock associations and geochemical compositions. Actually, there is a distinct difference for εHf(t) values of them: almost all the εHf(t) values of these magmatic rocks from the Nuru–Langshan Tectonic Zone are negative, while arc-related plutons from the Bainaimiao Arc have both positive and negative εHf(t) values (Fig. 12B, C). Thus we suggest that these early Paleozoic magmatic rocks from the Bainaimiao Arc are related to northward subduction of the South Bainaimiao Ocean. There may exist a Paleozoic cryptic suture zone between the North China Craton and the Nuru–Langshan Tectonic Zone (Dan et al. 2016). Detrital zircon age spectrums of the westernmost part of the Nuru–Langshan Tectonic Zone also show a close affinity to the South China Craton rather than the North China Craton (Song et al. 2017). Thus, the Nuru–Langshan Tectonic Zone and the North China Craton were likely to be separated by an ocean during early Paleozoic.

In short, our new data integrated with previous studies support a northward subduction of the South Bainaimiao Ocean which is a branch of the PAO during early Paleozoic. Meanwhile, there was an active continental margin for the Nuru–Langshan Tectonic Zone along the southern rim of the South Bainaimiao Ocean.

Tectonic evolution of the north margin of the North China Craton–Alxa region

Based on the above discussion and previously published data, the following updated tectono-paleogeographic model is proposed for early Paleozoic tectonic evolution along

the north margin of the North China Craton–Alxa region (Fig. 14).

To the east of the Gaqimaodu area, the northward subduction of the South Bainaimiao Ocean beneath the Bainaimiao Arc may start at late Cambrian as indicated by 499 ± 2 Ma arc-related meta-volcanic rocks (Zhang et al. 2019a). Chen et al. (2020) suggested that the ~ 518 Ma dacite reported by Zhang et al. (2014) was unrelated to development of the Bainaimiao Arc based on the abrupt change of the εHf(t) values. Numerous early Ordovician to late Silurian arc-related plutons and volcanic–(meta)sedimentary rocks are distributed in the Bainaimiao Arc (Chen et al. 2020; Qian et al. 2017; Zhang et al. 2019a, 2014, 2013b; Zhou et al. 2020). The early Silurian Xuniwusu Formation in the Bainaimiao area is considered as parts of an accretionary wedge by northward subduction of the South Bainaimiao Ocean. In the Ganqimaodu area, Zhang et al. (2015) reported a 475.8 ± 1.6 Ma pillow basalt within the ophiolitic mélanges. Moreover, the early Devonian sediments in this study were considered as flysch in an accretionary wedge by northward oceanic subduction. It indicates that the northward subduction of the South Bainaimiao Ocean was still ongoing during early Devonian in the study area as revealed by the MDAs of the accretionary sediments. The Southern Mongolia were likely an active margin evidenced by Ordovician volcanic and immature clastic rocks (Wu and He 1993) as well as Silurian intrusions (~ 423–434 Ma; Zheng et al. 2016) in the northern Alxa. The ~ 420 Ma peak of detrital zircon ages from the Devonian Yuanbaoshan Formation in the northern Alxa also shows that the Southern Mongolia was an active margin during late Silurian to early Devonian (Yin et al. 2015). All of these geological records indicate a continuous northward subduction of the South Bainaimiao Ocean from late Cambrian to early Devonian (~ 500–410 Ma). To the south of the South Bainaimiao Ocean, the northern North China Craton was possibly a passive continental margin with stable neritic clastic and carbonate deposition (Chen et al. 2015; Zhang et al. 2014), whereas the Nuru–Langshan Tectonic Zone was an active continental margin favored by ~ 460–407 Ma diorites and granites with depletions in Nb, Ta and negative εHf(t) values (Liu et al. 2016b; Teng et al. 2019; Tian et al. 2019a; Wang et al. 2015b). The Nuru–Langshan Tectonic Zone may be separated from the North China Craton by the branch of the South Bainaimiao Ocean. Although the time for final closure of the branch of the South Bainaimiao Ocean between the Nuru–Langshan Tectonic Zone and the North China Craton is still controversial, it should be later than late Devonian (Yuan and Yang 2015; Zhang et al. 2016a).

Previously most scholars suggested that early Devonian molasse deposition of Xibiehe Formation in the Bainaimiao Arc was the product of arc–continental collision (Chen et al. 2020; Xu et al. 2013; Zhang et al. 2014; Zhou et al. 2018b). However, all the detrital zircons of the Xibiehe Formation from the Bayan obo area and Bainaimiao area yield early Paleozoic ages without Precambrian ages (Chen et al. 2020; Wang et al. 2020). The sedimentary rocks from the Xibiehe Formation in the Jiefangyinzi area are dominated by Precambrian zircons, but their detrital zircon ages are different from those of the North China Craton (Ma et al. 2019). It is confusing why the North China Craton cannot provide detritus to the Xibiehe Formation if the molasse deposition is related to collision between the Bainaimiao Arc and the North China Craton. Therefore, the tectonic setting of the Xibiehe Formation needs to be confirmed by further study.

To sum up, we suggest that there exist bidirectional subduction for the western segment of the South Bainaimiao Ocean while the eastern part of it subducted beneath the Bainaimiao Arc to the north during late Cambrian to early Devonian (Fig. 14).

Conclusions

(1) Two quartz schists from the Ondor sum Group strata have maximum depositional ages of 412.3 ± 5.5 Ma and 417.7 ± 2.3 Ma, and three (meta)sandstones from the Hadahushu Group strata yield maximum depositional ages of 419.5 ± 2.8 Ma, 424.8 ± 5.0 Ma and 435.3 ± 5.9 Ma. New detrital zircon ages integrated with field data indicate that these two sets of strata were likely deposited in early Devonian.

(2) All samples from the early Devonian strata in the Ganqimaodu area have a prominent early Paleozoic age peak with extensive detrital zircons from Neoproterozoic to Archean. These early Paleozoic detrital zircons with both positive and negative εHf(t) values indicate intense magmatism derived from partial melt of the juvenile and recycled ancient crust at that time. The early Devonian strata in the Ganqimaodu area were parts of an accretionary complex containing ophiolitic mélanges. Arc-related plutons and preexisting basement in the Bainaimiao Arc were the main sources for these strata.

(3) Our new data supported a northward subduction of the South Bainaimiao Ocean in the Ganqimaodu region. An east–west-trending north-dipping subduction zone existed along the Bainaimiao Arc and the Southern Mongolia during late Cambrian to early Devonian.

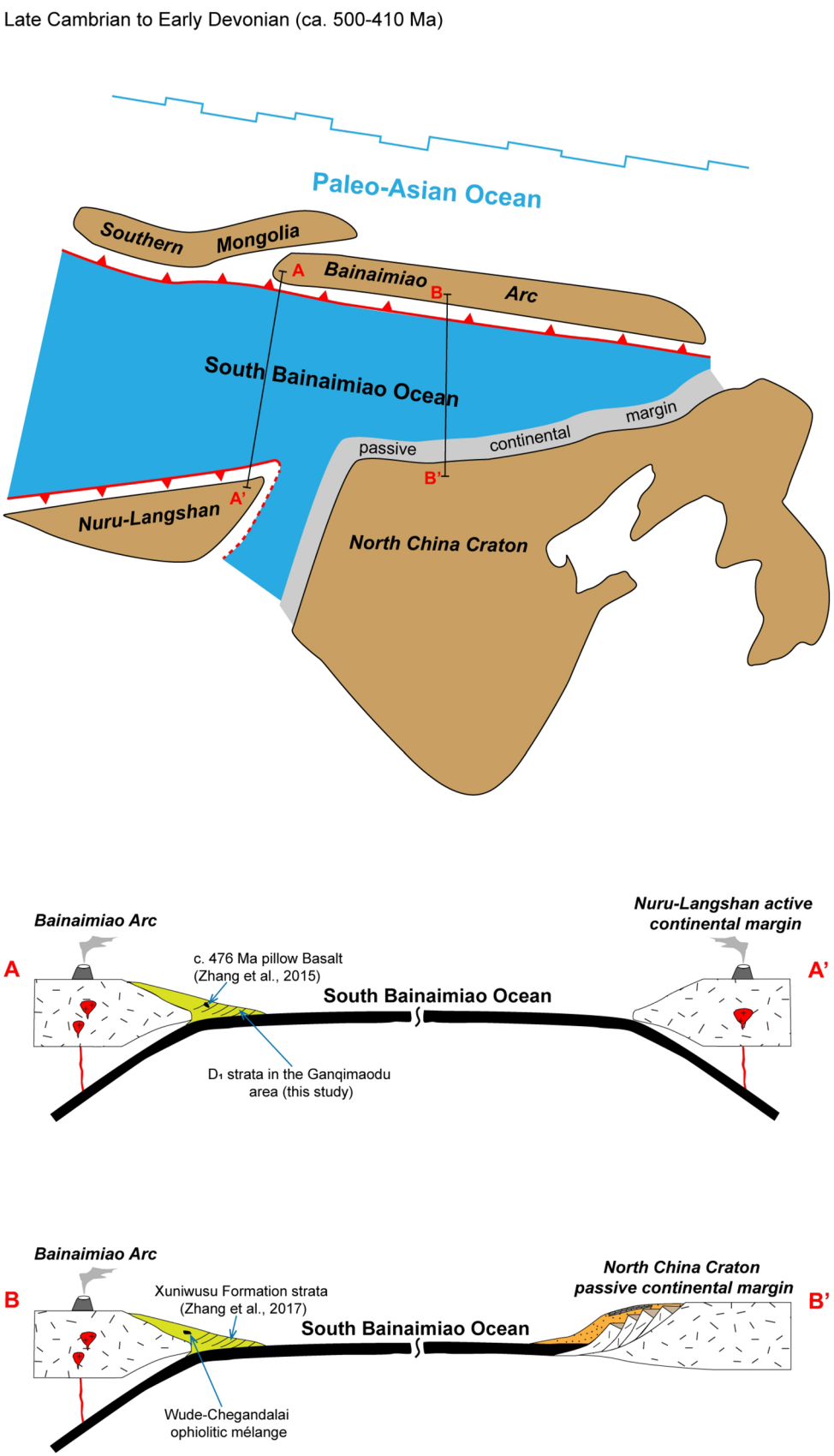

Fig. 14 Schemas showing the Early Paleozoic tectono-paleogeographic evolutional model for the northern margin of the North China Craton–Alxa region in the Southern Central Asian Orogenic Belt

Supplementary Information The online version contains supplementary material available at https://doi.org/10.1007/s00531-021-02148-z.

Acknowledgements We greatly appreciate the constructive comments from the journal editor and two reviewers, which led to major improvements in the quality of the paper. This work was funded by the National Natural Science Foundation of China (41730210, 41888101, 41672219), the Strategic Priority Research Program (B) of the Chinese Academy of Sciences (XDB26020301), the State Key R&D Program of China (2017YFC0601206), and the Youth Innovation Promotion Association CAS (2021062). This is a contribution to IGCP 662 & 669.

References

Andersen T (2002) Correction of common lead in U-Pb analyses that do not report 204Pb. Chem Geol 192:59–79

Anonymous (1980a) Geological Map of the Bayinhanggai Region, China, 1:200000, No. 1 Geological Survey Team of Inner Mongolia Autonomous Region (in Chinese)

Anonymous (1980b) Geological Map of the Xibo Region, China, 1:200000, No. 1 Geological Survey Team of Inner Mongolia Autonomous Region (in Chinese)

Badarch G, Dickson Cunningham W, Windley BF (2002) A new terrane subdivision for Mongolia: implications for the Phanerozoic crustal growth of Central Asia. J Asian Earth Sci 21:87–110

Bao C, Chen Y, Zhu X, Zhao J (2019) Attribution of the Langshan tectonic belt: evidence from zircon U-Pb ages and Hf isotope compositions. Geosci Front 10:539–551

Blichert-Toft J, Albarède F (1997) The Lu-Hf isotope geochemistry of chondrites and the evolution of the mantle-crust system. Earth Planet Sci Lett 148:243–258

Cawood PA, Kröner A, Collins WJ, Kusky TM, Mooney WD, Windley BF (2009) Accretionary orogens through Earth history. Geol Soc Lond Spec Publ 318:1–36

Cawood PA, Hawkesworth CJ, Dhuime B (2012) Detrital zircon record and tectonic setting. Geology 40:875–878

Chen X, Mou C, Zhou K, Kang J, Wang Q, Ge X, Liang W (2015) Sedimentary facies and palaeogeography of the North China region during the Ordovician (in Chinese with English abstract). Sediment Geol Tethyan Geol 35:1–11

Chen Y, Wu TR, Gan LS, Zhang ZC, Fu B (2019) Provenance of the early to mid-Paleozoic sediments in the northern Alxa area: implications for tectonic evolution of the southwestern Central Asian Orogenic Belt. Gondwana Res 67:115–130

Chen Y, Zhang Z, Qian X, Li J, Ji Z, Wu T (2020) Early to mid-Paleozoic magmatic and sedimentary records in the Bainaimiao Arc: an advancing subduction-induced terrane accretion along the northern margin of the North China Craton. Gondwana Res 79:263–282

Condie KC (2007) Accretionary orogens in space and time. In: 4-D Framework of Continental Crust. pp 145–158

Dan W, Li XH, Guo JH, Liu Y, Wang XC (2012) Paleoproterozoic evolution of the eastern Alxa Block, westernmost North China: evidence from in situ zircon U-Pb dating and Hf-O isotopes. Gondwana Res 21:838–864

Dan W, Li XH, Wang Q, Tang GJ, Liu Y (2014a) An Early Permian (ca. 280 Ma) silicic igneous province in the Alxa Block, NW China: A magmatic flare-up triggered by a mantle-plume? Lithos 204:144–158

Dan W, Li XH, Wang Q, Wang XC, Liu Y (2014b) Neoproterozoic S-type granites in the Alxa Block, westernmost north China and tectonic implications: In situ zircon U-Pb-Hf-O isotopic and geochemical constraints. Am J Sci 314:110–153

Dan W, Li XH, Wang Q, Wang XC, Wyman DA, Liu Y (2016) Phanerozoic amalgamation of the Alxa Block and North China Craton: evidence from Paleozoic granitoids, U-Pb geochronology and Sr-Nd-Pb-Hf-O isotope geochemistry. Gondwana Res 32:105–121

Demoux A, Kröner A, Liu D, Badarch G (2009) Precambrian crystalline basement in southern Mongolia as revealed by SHRIMP zircon dating. Int J Earth Sci 98:1365–1380

Dickinson WR, Gehrels GE (2009) Use of U-Pb ages of detrital zircons to infer maximum depositional ages of strata: a test against a Colorado Plateau Mesozoic database. Earth Planet Sci Lett 288:115–125

Fei MM, Pan M, Xie CL, Wang JH, Zhao HS (2019) Timing and tectonic settings of the Late Paleozoic intrusions in the Zhusileng, northern Alxa: implication for the metallogeny. Geosci J 23:37–57

Feng JY, Xiao WJ, Windley BF, Han CM, Wan B, Zhang J, Ao SJ, Zhang ZY, Lin LN (2013) Field geology, geochronology and geochemistry of mafic-ultramafic rocks from Alxa, China: implications for Late Permian accretionary tectonics in the southern Altaids. J Asian Earth Sci 78:114–142

Gehrels G (2014) Detrital zircon U-Pb Geochronology applied to tectonics. Annu Rev Earth Planet Sci 42:127–149

Geng YS, Zhou X (2010) Early Neoproterozoic granite events in Alax area of Inner Mongol ia and their geological significance: evidence from geochronology (in Chinese with English abstract). Acta Petrologica Et Mineralogica 29:779–795

Gong JH, Zhang JX, Wang ZQ, Yu SY, Li HK, Li YS (2016) Origin of the Alxa Block, western China: new evidence from zircon U-Pb geochronology and Hf isotopes of the Longshoushan Complex. Gondwana Res 36:359–375

Griffin WL, Pearson NJ, Belousova E, Jackson SE, Van Achterbergh E, O'Reilly SY, Shee SR (2000) The Hf isotope composition of cratonic mantle: LAM-MC-ICPMS analysis of zircon megacrysts in kimberlites. Geochim Cosmochim Acta 64:133–147

Griffin WL, Wang X, Jackson SE, Pearson NJ, O'Reilly SY, Xu X, Zhou X (2002) Zircon chemistry and magma mixing, SE China: in-situ analysis of Hf isotopes, Tonglu and Pingtan igneous complexes. Lithos 61:237–269

Guy A, Schulmann K, Clauer N, Hasalová P, Seltmann R, Armstrong R, Lexa O, Benedicto A (2014) Late Paleozoic-Mesozoic tectonic evolution of the Trans-Altai and South Gobi Zones in southern Mongolia based on structural and geochronological data. Gondwana Res 25:309–337

He J, Zhu W, Ge R (2014a) New age constraints on Neoproterozoic diamicites in Kuruktag, NW China and Precambrian crustal evolution of the Tarim Craton. Precambr Res 241:44–60

He J, Zhu W, Ge R, Zheng B, Wu H (2014b) Detrital zircon U-Pb ages and Hf isotopes of Neoproterozoic strata in the Aksu area, northwestern Tarim Craton: implications for supercontinent reconstruction and crustal evolution. Precambr Res 254:194–209

Hou K, Li Y, Zou T, Qu X, Shi Y, Xie G (2007) Laser ablation-MC-ICP-MS technique for Hf isotope microanalysis of zircon and its geological applications (in Chinese with English abstract). Acta Petrol Sinica 23:2595–2604

Hu S (2019) The geological significance of the early paleozoic mélange in Chegandalai, Inner Mongolia (in Chinese with English abstract). Master thesis, China University of Geoscience (Beijing)

Hu JM, Gong WB, Wu SJ, Liu Y, Liu SC (2014) LA-ICP-MS zircon U-Pb dating of the Langshan Group in the northeast margin of the Alxa block, with tectonic implications. Precambr Res 255:756–770

Iizuka T, Hirata T (2005) Improvements of precision and accuracy in in situ Hf isotope microanalysis of zircon using the laser ablation-MC-ICPMS technique. Chem Geol 220:121–137

Jahn BM, Wu FY, Chen B (2000) Granitoids of the Central Asian Orogenic Belt and continental growth in the Phanerozoic. Trans R Soc Edinb Earth Sci 91:181–193

Jia H, Baoyin W, Zhang Y (2003) Characteristics and tectonic significance of the Wude suture zone in northern Damaoqi, Inner Mongolia (in Chinese with English abstract). J Chengdu Univ Technol (Sci Technol Ed) 30:30–34

Jian P, Liu D, Kröner A, Windley BF, Shi Y, Zhang F, Shi G, Miao L, Zhang W, Zhang Q, Zhang L, Ren J (2008) Time scale of an early to mid-Paleozoic orogenic cycle of the long-lived Central Asian Orogenic Belt, Inner Mongolia of China: implications for continental growth. Lithos 101:233–259

Khain EV, Bibikova EV, Kröner A, Zhuravlev DZ, Sklyarov EV, Fedotova AA, Kravchenko-Berezhnoy IR (2002) The most ancient ophiolite of the Central Asian fold belt: U-Pb and Pb–Pb zircon ages for the Dunzhugur Complex, Eastern Sayan, Siberia, and geodynamic implications. Earth Planet Sci Lett 199:311–325

Kröner A, Windley BF, Badarch G, Tomurtogoo O, Hegner E, Jahn BM, Gruschka S, Khain EV, Demoux A, Wingate MTD (2007) Accretionary growth and crust formation in the Central Asian Orogenic Belt and comparison with the Arabian-Nubian shield. In: 4-D Framework of Continental Crust. pp 181–209

Lehmann J, Schulmann K, Lexa O, Corsini M, Kröner A, Stipska P, Tomurhuu D, Otgonbator D (2010) Structural constraints on the evolution of the Central Asian Orogenic Belt in SW Mongolia. Am J Sci 310:575–628

Li C, Ran H, Zhao L, Wang H, Zhang K, Xu Y, Gu Y, Zhang Y (2012) LA-MC-ICPMS U-Pb geochronology of zircons from the Wenduermiao Group and its tectonic significance (in Chinese with English abstract). Acta Petrol Sinica 28:3705–3714

Li Z, Qiu N, Chang J, Yang X (2015) Precambrian evolution of the Tarim Block and its tectonic affinity to other major continental blocks in China: new clues from U-Pb geochronology and Lu–Hf isotopes of detrital zircons. Precambr Res 270:1–21

Liu Y (2012) Geochemical and chronological characteristics of granitic gneisses and intrusive rocks from dongshengmiao region, Inner Mongolia and Their Tectonic Implications (in Chinese with English abstract). Master thesis, Lanzhou University

Liu D, Jian P, Zhang Q, Zhang F, Shi Y, Shi G, Zhang N, Tao H (2003) SHRIMP dating of Adakites in the Tulingkai Ophiolite, Inner Mongolia: evidence for the early Paleozoic subduction (in Chinese with English abstract). Acta Geol Sinica 77:317–327

Liu JF, Li J, Chi X, Feng Q, Hu ZC, Zhou K (2013) Early Devonian felsic volcanic rocks related to the arc-continent collision on the northern margin of North China craton–evidences of zircon U-Pb dating and geochemical characteristics (in Chinese with English abstract). Geol Bull China 32:267–278

Liu M, Zhang D, Xiong G, Zhao H, Di Y, Wang Z, Zhou Z (2016a) Zircon U-Pb age, Hf isotope and geochemistry of Carboniferous intrusions from the Langshan area, Inner Mongolia: petrogenesis and tectonic implications. J Asian Earth Sci 120:139–158

Liu Q, Zhao GC, Sun M, Han YG, Eizenhofer PR, Hou WZ, Zhang XR, Zhu YL, Wang B, Liu DX, Xu B (2016b) Early Paleozoic subduction processes of the Paleo-Asian Ocean: insights from geochronology and geochemistry of Paleozoic plutons in the Alxa Terrane. Lithos 262:546–560

Liu C, Zhao G, Liu F, Shi J (2017a) Detrital zircon U-Pb and Hf isotopic and whole-rock geochemical study of the Bayan Obo Group, northern margin of the North China Craton: implications for Rodinia reconstruction. Precambr Res 303:372–391

Liu Q, Zhao GC, Han YG, Eizenhofer PR, Zhu YL, Hou WZ, Zhang XR (2017b) Timing of the final closure of the Paleo-Asian Ocean in the Alxa Terrane: constraints from geochronology and geochemistry of Late Carboniferous to Permian gabbros and diorites. Lithos 274:19–30

Liu CH, Zhao GC, Liu FL, Shi JR (2019a) Late Precambrian tectonic affinity of the Alxa block and the North China Craton: evidence from zircon U-Pb dating and Lu-Hf isotopes of the Langshan Group. Precambr Res 326:312–332

Liu Y, Wang W, Teng X, Guo S, He P, Tian J, Duan X (2019b) Geochemistry and Hf Isotopes Characteristics and Geological Significance of Latest Early Permian Granodiorite of Langshan Area, Inner Mongolia (in Chinese with English abstract). Adv Earth Sci 34:366–381

Liu M, Lai SC, Zhang D, Zhu RZ, Qin JF, Xiong GQ, Wang HR (2020) Constructing the latest Neoproterozoic to early Paleozoic multiple crust-mantle interactions in western Bainaimiao arc terrane, southeastern Central Asian Orogenic Belt. Geosci Front 11:1727–1742

Ludwig KR (2003) ISOPLOT 3.00: a geochronological toolkit for microsoft excel. Berkeley Geochronology Center, California, Berkeley

Ma S, Wang Z, Zhang Y, Sun J (2019) Bainaimiao Arc as an Exotic Terrane Along the Northern Margin of the North China Craton: Evidences from petrography, Zircon U-Pb dating, and geochemistry of the early devonian deposits. Tectonics 38:2606–2624

Peng R, Zhai Y, Wang J, Chen X, Liu QLJ, Shi Y, Wang G, Li S, Wang L, Ma Y, Zhang P (2010) Discovery of neoproterozoic acid volcanic rock in the western section of Langshan, Inner Mongolia, and its geological significance (in Chinese with English abstract). Chin Sci Bull 55:2611–2620

Qian X, Zhang Z, Chen Y, Yu H, Luo Z, Yang J (2017) Geochronology and geochemistry of early Paleozoic Igneous Rocks in Zhurihe Area, Inner Mongolia and Their Tectonic Significance (in Chinese with English abstract). Earth Sci 42:1472–1494

Rojas-Agramonte Y, Kröner A, Demoux A, Xia X, Wang W, Donskaya T, Liu D, Sun M (2011) Detrital and xenocrystic zircon ages from Neoproterozoic to Palaeozoic arc terranes of Mongolia: significance for the origin of crustal fragments in the Central Asian Orogenic Belt. Gondwana Res 19:751–763

Safonova I, Kotlyarov A, Krivonogov S, Xiao W (2017) Intra-oceanic arcs of the Paleo-Asian Ocean. Gondwana Res 50:167–194

Şengör AMC, Natal'in BA (1996) Turkic-type orogeny and its role in the making of the continental crust. Ann Rev EarthPlanet Sci 24(1):263–337

Şengör AMC, Natal'in BA, Burtman VS (1993) Evolution of the Altaid tectonic collage and Palaeozoic crustal growth in Eurasia. Nature 364:299–307

Shang H, Tao J, Baoyin W, Hao X (2003) The arc-basin system and tectonic significance of early Paleozoic in Baiyun' ebo Area Inner Mongolia. Geol Surv Res 26:160–168

Shen Q, Geng YS, Wang X, Wu CM (2005) Petrology, geochemistry, formation environment and ages of Precambrian amphibolites in Alxa region (in Chinese with English abstract). Acta Petrologica Et Mineralogica 24:21–31

Shi G, Faure M, Xu B, Zhao P, Chen Y (2013) Structural and kinematic analysis of the Early Paleozoic Ondor Sum-Hongqi mélange belt, eastern part of the Altaids (CAOB) in Inner Mongolia, China. J Asian Earth Sci 66:123–139

Shi XJ, Wang T, Zhang L, Castro A, Xiao XC, Tong Y, Zhang JJ, Guo L, Yang QD (2014) Timing, petrogenesis and tectonic setting of the Late Paleozoic gabbro-granodiorite-granite intrusions in the Shalazhashan of northern Alxa: constraints on the southernmost boundary of the Central Asian Orogenic Belt. Lithos 208:158–177

Shi XJ, Zhang L, Wang T, Zhang J, Liu M, Zhou H, Yan YT (2016) Zircon geochronology and Hf isotopic compositions for the

Mesoproterozoic gneisses in Zongnaishan area, northern Alxa and its tectonic affinity (in Chinese with English abstract). Acta Petrol Sinica 32:3518–3536

Shi GZ, Wang H, Liu ET, Huang CY, Zhao JX, Song GZ, Liang C (2018) Sr-Nd-Pb isotope systematics of the Permian volcanic rocks in the northern margin of the Alxa Block (the Shalazhashan Belt) and comparisons with the nearby regions: Implications for a Permian rift setting? J Geodyn 115:43–56

Söderlund U, Patchett PJ, Vervoort JD, Isachsen CE (2004) The 176Lu decay constant determined by Lu–Hf and U-Pb isotope systematics of Precambrian mafic intrusions. Earth Planet Sci Lett 219:311–324

Song DF, Xiao WJ, Collins AS, Glorie S, Han CM, Li YC (2017) New chronological constrains on the tectonic affinity of the Alxa Block, NW China. Precambr Res 299:230–243

Song DF, Xiao WJ, Collins AS, Glorie S, Han CM, Li YC (2018) Final subduction processes of the Paleo-Asian Ocean in the Alxa Tectonic Belt (NW China): constraints from field and chronological data of permian Arc-related volcano-sedimentary rocks. Tectonics 37:1658–1687

Song DF, Xiao WJ, Collins AS, Glorie S, Han CM (2019) Late Carboniferous-early Permian arc magmatism in the south-western Alxa Tectonic Belt (NW China): constraints on the late Palaeozoic subduction history of the Palaeo-Asian Ocean. Geol J 54:1046–1063

Sun L, Zhao F, Wang H, Ren B, Peng S, Teng F (2013) Zircon U-Pb geochronology of metabase rocks from the Baoyintu Block in the Langshan Area, inner Mongolia, and Its Tectonic Signification (in Chinese with English abstract). Acta Geol Sinica 87:197–207

Sun L, Zhang Y, Hu X, Ren B, Wang S, Zhang T (2018) Geochemical characteristics and zircon U-Pb geochronology of Paleoproterozoic metamorphic granites from northern Langshan, Inner Mongolia: magmatic response to the breakup of Columbia supercontinent (in Chinese with English abstract). Acta Petrol Sinica 34:3116–3136

Taylor J, Webb L, Johnson C, Heumann M (2013) The lost south gobi microcontinent: protolith studies of metamorphic tectonites and implications for the evolution of continental crust in southeastern Mongolia. Geosciences 3:543–584

Teng X, Tian J, Liu Y, Zhang Y, Teng F, Duan X (2019) Definition and geological significance of early silurian quartz diorite in Langshan Area, Inner Mongolia (in Chinese with English abstract). Earth Sci 44:1236–1252

Tian J, Teng X, Zhang Y, Liu Y, Duan X (2019a) The discovery of Late Silurian quartz diorite in Langshan area of Inner Mongolia and its geological implications (in Chinese with English abstract). Geol Bull China 38:1158–1169

Tian J, Xin H, Teng X, Liu Y, Guo S, Teng F, He P, Wang W (2019b) Tectonic siginificance of carbonniferous-triassic Magmatism in Langshan Area, Inner Mongolia (in Chinese with English abstract). Earth Sci 44:206–219

Tian J, Zhang Y, Teng X, Liu Y, Teng F, Guo S, He P, Wang W (2019c) The determination of Late Silurian two-mica monzonitic pluton in the Langshan area, Inner Mongolia and its geological implication (in Chinese with English abstract). Acta Geol Sinica 93:661–673

Tian RS, Xie GA, Zhang J, Zhu WB, Qu JF, Gao S (2019d) Sedimentary provenance and age of the Langshan Group in the northeastern Alxa Block: implications for Neoproterozoic tectonic evolution. Int J Earth Sci 108:1705–1723

Tian Y, Xu B, Zhang Y, Yang Z, Yao Z (2019e) Sedimentary facies and provenance area analysis of Xuniwusu Formation in Tugurige Area, southern xing-meng orogenic belt and their tectonic significance. Acta Sci Natl Univ Pekinen (Chin Engl Abstr) 55:1038–1054

Vermeesch P (2012) On the visualisation of detrital age distributions. Chem Geol 312–313:190–194

Wang T, Zheng Y, Gehrels G, Mu Z (2001) Chronology evidence of south Mongolia existed: zircon U-Pb ages of the Yagan-Wengqihaierhan core complex granitic gneiss. Chin Sci Bull 46:1220–1223

Wang W, Liu S, Santosh M, Deng Z, Guo B, Zhao Y, Zhang S, Yang P, Bai X, Guo R (2015a) Late Paleoproterozoic geodynamics of the North China Craton: geochemical and zircon U-Pb–Hf records from a volcanic suite in the Yanliao rift. Gondwana Res 27:300–325

Wang ZZ, Han BF, Feng LX, Liu B (2015b) Geochronology, geochemistry and origins of the Paleozoic-Triassic plutons in the Langshan area, western Inner Mongolia, China. J Asian Earth Sci 97:337–351

Wang ZW, Pei FP, Xu WL, Cao HH, Wang ZJ, Zhang Y (2016a) Tectonic evolution of the eastern Central Asian Orogenic Belt: evidence from zircon U-Pb–Hf isotopes and geochemistry of early Paleozoic rocks in Yanbian region, NE China. Gondwana Res 38:334–350

Wang ZZ, Han BF, Feng LX, Liu B, Zheng B, Kong LJ (2016b) Tectonic attribution of the Langshan area in western Inner Mongolia and implications for the Neoarchean-Paleoproterozoic evolution of the Western North China Craton: Evidence from LA-ICP-MS zircon U-Pb dating of the Langshan basement. Lithos 261:278–295

Wang S, Li S, Li W, Xu Z, Zhang J, Li C, Shi Q, Liu Y, Wang W, Guan Q (2020) Tectonic evolution of southeast central Asian Orogenic Belt: evidence from geochronological data and paleontology of the early Paleozoic deposits in Inner Mongolia. J Earth Sci 31:743–756

Windley BF, Alexeiev D, Xiao WJ, Kröner A, Badarch G (2007) Tectonic models for accretion of the Central Asian Orogenic Belt. J Geol Soc Lond 164:31–47

Wu TR, He GQ (1993) Tectonic units and their fundamental characteristics on the northern margin of the Alxa Block (in Chinese with English abstract). Acta Geol Sinica 67:97–108

Wu FY, Yang YH, Xie LW, Yang JH, Xu P (2006) Hf isotopic compositions of the standard zircons and baddeleyites used in U-Pb geochronology. Chem Geol 234:105–126

Wu F, Yang J, Wilde S, Liu X, Guo J, Zhai M (2007) Detrital zircon U-Pb and Hf isotopic constraints on the crustal evolution of North Korea. Precambr Res 159:155–177

Wu SJ, Hu JM, Ren MH, Gong WB, Liu Y, Yan JY (2014) Petrography and zircon U-Pb isotopic study of the Bayanwulashan Complex: constrains on the Paleoproterozoic evolution of the Alxa Block, westernmost North China Craton. J Asian Earth Sci 94:226–239

Xiao WJ, Windley BF, Hao J, Zhai M (2003) Accretion leading to collision and the Permian Solonker suture, Inner Mongolia, China: Termination of the central Asian orogenic belt. Tectonics 22:8/1–8/20

Xiao WJ, Windley BF, Huang BC, Han CM, Yuan C, Chen HL, Sun M, Sun S, Li JL (2009) End-Permian to mid-Triassic termination of the accretionary processes of the southern Altaids: implications for the geodynamic evolution, Phanerozoic continental growth, and metallogeny of Central Asia. Int J Earth Sci 98:1189–1217

Xiao WJ, Windley BF, Allen MB, Han C (2013) Paleozoic multiple accretionary and collisional tectonics of the Chinese Tianshan orogenic collage. Gondwana Res 23:1316–1341

Xiao WJ, Windley BF, Sun S, Li J, Huang B, Han C, Yuan C, Sun M, Chen H (2015a) A tale of amalgamation of three permo-triassic collage systems in Central Asia: oroclines, sutures, and terminal accretion. Annu Rev Earth Planet Sci 43:477–507

Xiao Z, Kang J, Wang H, Gao Z, Xiang Z, Chu H, Ren Y (2015b) Formation age of Alxa group-complex (Special) in Alxa Area,

Inner Mongolia (in Chinese with English abstract). Geol Surv Res 38:182–191

Xie L, Zhang Y, Zhang H, Sun J, Wu F (2008) In situ simultaneous determination of trace elements, U-Pb and Lu-Hf isotopes in zircon and baddeleyite. Sci Bull 53:1565–1573

Xu B, Charvet J, Chen Y, Zhao P, Shi G (2013) Middle Paleozoic convergent orogenic belts in western Inner Mongolia (China): framework, kinematics, geochronology and implications for tectonic evolution of the Central Asian Orogenic Belt. Gondwana Res 23:1342–1364

Xu B, Xu Y, Li J, Li Q (2016) Age of the Ondor sum Group in western Inner Mongolia and its position in the Central Asia Orogenic Belt (in Chinese with English abstract). Earth Sciences Frontiers (China University of Geosciences (Beijing); Peking University) 23:120–127

Yarmolyuk VV, Kovalenko VI, Sal'nikova EB, Kozakov IK, Kotov AB, Kovach VP, Vladykin NV, Yakovleva SZ (2005) U-Pb age of syn- and postmetamorphic granitoids of South Mongolia: evidence for the presence of grenvillides in the central Asian foldbelt. Dokl Earth Sci 404:986–990

Yin H, Zhou H, Cheng R, Zhang W, Zheng X, Yang L, Wang S (2015) The age, sedimentary characteristics and tectonic significance on the Yuanbaoshan Formation in the Southern Margin of the Siberian Plate, North of Alxa, Inner Mongolia (in Chinese with English abstract). Acta Sedimentol Sin 33:665–678

Yin HQ, Zhou HR, Zhang WJ, Zheng XM, Wang SY (2016) Late Carboniferous to early Permian sedimentary-tectonic evolution of the north of Alxa, Inner Mongolia, China: evidence from the Amushan Formation. Geosci Front 7:733–741

Yin H (2016) Late Paleozoic sedimentary characteristics and its tectonic evolution in Northern Alxa area, Inner Mongolia (in Chinese with English abstract). Ph.D. thesis, China University of Geosciences (Beijing)

Yuan W, Yang Z (2015) The Alashan Terrane did not amalgamate with North China block by the Late Permian: evidence from Carboniferous and Permian paleomagnetic results. J Asian Earth Sci 104:145–159

Zhang YP, Su Y, Li J (2010) Regional tectonics significance of the Late Silurian Xibiehe Formation in central Inner Mongolia, China (in Chinese with English abstract). Geol Bull China 29:1599–1605

Zhang JX, Gong JH, Yu SY, Li HK, Hou KJ (2013a) Neoarchean-Paleoproterozoic multiple tectonothermal events in the western Alxa block, North China Craton and their geological implication: evidence from zircon U-Pb ages and Hf isotopic composition. Precambr Res 235:36–57

Zhang W, Jian P, Kröner A, Shi Y (2013b) Magmatic and metamorphic development of an early to mid-Paleozoic continental margin arc in the southernmost Central Asian Orogenic Belt, Inner Mongolia, China. J Asian Earth Sci 72:63–74

Zhang W, Wu TR, Feng JC, Zheng RG, He YK (2013c) Time constraints for the closing of the Paleo-Asian Ocean in the Northern Alxa Region: Evidence from Wuliji granites. Sci China Earth Sci 56:153–164

Zhang SH, Zhao Y, Ye H, Liu JM, Hu ZC (2014) Origin and evolution of the Bainaimiao arc belt: implications for crustal growth in the southern Central Asian orogenic belt. Geol Soc Am Bull 126:1275–1300

Zhang H, Zhang Y, Gao X, Li X, Zhang J, Xing W, Jiao S, Guo B, Liu B, Zhang G (2015) Geological characteristics and zircon U-Pb age of pillow basalt of ophiolitic mélange in Wenqigenwulan, Inner Mongolia (in Chinese with English abstract). Geol Bull China 34:1878–1883

Zhang J, Zhang BH, Zhao H (2016a) Timing of amalgamation of the Alxa Block and the North China Block: constraints based on detrital zircon U-Pb ages and sedimentologic and structural evidence. Tectonophysics 668:65–81

Zhang W, Pease V, Meng QP, Zheng RG, Thomsen TB, Wohlgemuth-Ueberwasser C, Wu TR (2016b) Discovery of a Neoproterozoic granite in the Northern Alxa region, NW China: its age, petrogenesis and tectonic significance. Geol Mag 153:512–523

Zhang J, Liu Z, Guan Q, Xu Z, Wang X, Zhu K (2017a) Age and geological significance of Xuniwusu Formation from Bainaimiao area of Sonid Youqi, Inner Mongolia (in Chinese with English abstract). Acta Petrologica Sinica 33:3147–3160

Zhang W, Pease V, Meng QP, Zheng RG, Wu TR, Chen Y, Gan LS (2017b) Age and petrogenesis of late Paleozoic granites from the northernmost Alxa region, northwest China, and implications for the tectonic evolution of the region. Int J Earth Sci 106:79–96

Zhang C, Quan J, Liu Z, Xu Z, Pang X, Zhang Y (2019a) Geochemical characteristics and geological significance of meta-volcanic rocks of the Bainaimiao group, Sonid Right Banner, Inner Mongolia, China. J Earth Sci 30:272–285

Zhang Y, Sun L, Zhang T, Teng F, Zhang Y, Sun Y, Yang Z, Xu F (2019b) Geochronology, geochemistry and its tectonic significance of the early Paleozoic magmatic rocks in Northern Langshan, Inner Mongolia. Earth Sci 44:179–192

Zhao Y, Zhai M, Chen H, Zhang SH (2017) Paleozoic-early Jurassic tectonic evolution of North China Craton and its adjacent orogenic belts (in chinese with English abstract). Geol China 44:44–60

Zheng RG, Wu TR, Zhang W, Feng JC, Xu C, Meng QP, Zhang Z (2013) Geochronology and geochemistry of the Yagan granite in the northern margin of the Alxa block: constraints on the tectonic evolution of the southern Altaids (in Chinese with English abstract). Acta Petrologica Sinica 29:2665–2675

Zheng RG, Wu TR, Zhang W, Xu C, Meng QP, Zhang ZY (2014) Late Paleozoic subduction system in the northern margin of the Alxa block, Altaids: geochronological and geochemical evidences from ophiolites. Gondwana Res 25:842–858

Zheng RG, Li J, Xiao W, Liu J, Wu TR (2016) Discovery of Silurian Pluton in the Enger Us Region in the Northern Margin of Alxa Block. Acta Geol Sinica 90:1725–1736

Zheng B, Zhu W, Ge R, Wu H, He J, Lu Y (2020) Proterozoic tectonic evolution of the Tarim Craton: New insights from detrital zircon U-Pb and Lu-Hf isotopes of metasediments in the Kuruktag area. Precamb Res 346:105788

Zhou YZ, Han BF, Xu Z, Ren R, Su L (2013) The age of the Proterozoic rocks in Yingba area in western Inner Mongolia: Constraints on the distribution of the South Gobi micro-continent in the Central Asian orogenic belt (in Chinese with English abstract). Geol Bull China 32:318–326

Zhou H, Pei FP, Zhang Y, Zhou ZB, Xu WL, Wang ZW, Cao HH, Yang C (2018a) Origin and tectonic evolution of early Paleozoic arc terranes abutting the northern margin of North China Craton. Int J Earth Sci 107:1911–1933

Zhou H, Zhao G, Han Y, Wang B (2018b) Geochemistry and zircon U-Pb-Hf isotopes of Paleozoic intrusive rocks in the Damao area in Inner Mongolia, northern China: Implications for the tectonic evolution of the Bainaimiao arc. Lithos 314–315:119–139

Zhou JB, Wilde SA, Zhao GC, Han J (2018c) Nature and assembly of microcontinental blocks within the Paleo-Asian Ocean. Earth Sci Rev 186:76–93

Zhou H, Zhao G, Han Y, Wang B, Pei X (2020) Tectonic origin of the Bainaimiao arc terrane in the southern Central Asian orogenic belt: evidence from sedimentary and magmatic rocks in the Damao region. GSA Bull 133:802–818

Zhu GY, Chen ZY, Chen WY, Yan HH, Zhang PH (2021) Revisiting to the Neoproterozoic tectonic evolution of the Tarim Block, NW China. Precamb Res 352:106013